Latin American Journal of Solids and Structures
www.lajss.org

Viscoelastic Substrates Effects on the Elimination or Reduction of the Sandwich Structures Oscillations Based on the Kelvin-Voigt Model

Abstract

Effects of viscoelastic substrates on the sandwich structures oscillations are examined in this paper. In this regard, dynamic response of sandwich annular panels with FG polar orthotropic face sheets resting on viscoelastic substrate is presented. Young's modulus in the radial and circumferential direction, shear modulus and density of each face sheet may be varied continuously in the radial direction. The viscoelastic substrate is modeled as Kelvin-Voigt foundation. To describe more accurately response of sandwich structures, the governing dynamical equations are derived based on the layer-wise theory and five systems of second order coupled partial differential equations are obtained. The effects of the stiffness and damping coefficients of the foundation on the dynamic behavior of sandwich plate are investigated for various transient loads and boundary condition. Since no available results may be found in literature to demonstrate the efficiency and accuracy of the obtained results, the obtained results are verified by comparison with finite element results based on the three dimensional theory of elasticity for some special cases.

Keywords

Dynamic response; FG polar orthotropic; viscoelasticfoundation; transient loads, Kelvin-Voigt.

M.M. Alipour [a, *]
I. Rajabi [b]

[a] Assistant Professor, Department of Mechanical Engineering, University of Mazandaran, Babolsar 47416-13534, IranE-mail: m.mollaalipour@umz.ac.ir m.m.alipur@gmail.com
[b] Assistant Professor, Department of Mechanical Engineering, Malek Ashtar University, Shiraz, Iran.
E-mail: irajabi@mail.kntu.ac.ir

* Corresponding author

http://dx.doi.org/10.1590/1679-78254096

Received 07.06.2017
In revised form 29.08.2017
Accepted 04.09.2017
Available online 18.09.2017

1 INTRODUCTION

Sandwich structures are widely used in the industries. In practical applications, sandwich structures are subjected to various transient dynamic loads where reduce vibration of these structures under-dynamic loads is important in many engineering fields and viscoelastic substrate can be applied to reducethe vibration of structures. In addition, structures resting on viscous, elastic or viscoelastic foundationare extensively used in many engineering fields. However, most of the performed studies

arelimited to the static and free vibration analyses of sandwich plates and rare researches are available onthe dynamic analysis especially for plates under viscoelastic foundation.

The dynamic response of a plate of infinite extent on a viscous Winkler foundation subjected to movingtandem-axle loads with amplitude variation was investigated by Kim and McCullough (2003), based onthe classical plate theory. Liang et al. (2014) studied the transient response of functionally graded annularplate under a two parameter viscoelastic foundation based on the three-dimensional theory ofelasticity and using the differential quadrature method, state space method and Laplace transform.Vibration reduction of composite plates by piezoelectric patches was investigated by Bargh and Sadra (2014), based on the classical plate theory and using a modified artificial bee colony algorithm. Basedon the sinusoidal shear deformation theory and by using the Navier's and meshless methods, free vibrationanalyses of viscoelastic double-bonded polymeric nanocomposite plates are investigated byMohammadimehr et al. (2015). Forced vibration analysis of a single layer viscoelastic graphene sheetresting on viscoelastic medium was performed by Hosseini Hashemi et al. (2015). The governing equationis derived using Hamilton's principle based on the classical plate theory and viscoelastic KelvinVoigt model. Luong-Van et al. (2014) investigated the dynamic responses of sandwich and laminatedcomposite plates resting on viscoelastic foundation based on the first-order shear deformation theoryand finite element method. Arani et al. carried out the free vibration analysis of the coupled system ofdouble-layered rectangular (2012) and annular (2014) graphene sheets embedded in a visco-Pasternak foundation was by. The motion equations were derived based on the Hamilton's principleand first-order shear deformation theory. The differential quadrature method was applied to obtain thefrequency ratio for various boundary conditions. Lepoittevin and Kress (2011) proposed a method topredict resonance frequencies and modal loss factors of bare and damped samples, using constrainedlayer damping treatment, under free–free boundary condition. Karim and Chen (2012) investigated thesurface damping effects of anchored constrained viscoelastic layers on the flexural response of simplysupported Euler beams or plate strips under base excitations. In order to reduce the structural vibrationsof a mechanical system used in aerospace, a new sketch of eddy current damper (ECD) was proposedby Pan et al. (2016). Zenkour (2016) applied the classical plate theory and Fourier transformmethod for transient thermal analysis of a single layered graphene sheet embedded in viscoelastic medium.The governing dynamical equation was obtained and solved for simply-supported grapheme sheet. By using the Rayleigh–Ritz method, Plattenburg et al. (2016) proposed a new analytical modelfor a thin cylindrical shell that utilizes a homogeneous cardboard liner to increase modal damping. Theproposed theory, incorporated material structural damping along with frequency-dependent viscousand Coulomb interfacial damping formulations for the shell–liner interaction. By using the Galerkinweighted residual method and the classical plate theory, Kiasat et al. (2014) analyzed the transientresponse of viscoelastic beams and plates on viscoelastic medium. Based on Kelvin-Voigt model, freedamped vibration analysis of plates with hybrid material foundation viscoelasticity was performed by Zamani et al. (2017). Free vibration analysis of a simply supported viscoelastic orthotropic nanoplates resting on viscoelastic medium was studied by Pouresmaeeli et al. (2013), using the classical plate theoryand the Navier method. Zhang et al. (2016) analyzed the free transverse vibration of double walledcarbon nanotubes embedded in viscoelastic medium by using the Euler–Bernoulli beam theory. Luo etal. (2016) presented a closed-form solution to a viscoelastically supported Timoshenko

beam under aharmonic line load. The differential governing equations were converted into algebraic equations byassuming the deflection and rotation of the beam in harmonic forms with respect to time and space.Some researchers analyzed beams resting on viscoelastic foundations subjected to moving loads. Thevibration instability analysis of an oscillator moving along a Timoshenko beam was performed byMetrikine and Verichev (2001) and Mazilu et al. (2012). The inHluence of a nonlinear foundation on thedynamic response of a periodically supported beam was investigated by Hoang et al. (2016), based on the Euler–Bernoulli beam theory. Ding et al. (2013) investigated the dynamic response of infinitebeams supported by nonlinear viscoelastic foundations. The differential equations were obtained byemploying the Timoshenko beam theory and were solved based on the Adomian decomposition methodand a perturbation method in conjunction with complex Fourier transformation. The dynamic response of finite Timoshenko beamsresting on a six parameter foundation was studied by Yang et al. (2013).

Most of the existing researches were performed based on the equivalent single layer theories, whereusing the equivalent single-layer theories for analysis of sandwich plates may be inaccurate or erroneousin most circumstances. Various theories are presented for analysis of sandwich structure Carrera and Brischetto (2008).Many researchers investigated the laminated composite and sandwich plates based on the sandwichand multilayered structures theories. Thermoelastic bending of functionally graded sandwich plates were analyzed by Houari et al (2013) based on a new higher order shear and normal deformation theory and by Tounsi et al. (2013) based on A refined trigonometric shear deformation theory.Based on layerwise formulation, Alipour (2016a) presented anovel economical analytical method for bending and stress analysis of functionally graded sandwichcircular plates subjected to various loads with general elastic edge conditions. Alipour (2016b) analyzed the effects of elastically restrained edges on FG sandwich annular plates by using a novel solutionprocedure and layerwise method. Alipour (2018) examined the dynamic response of sandwich plate with viscoelastic boundary support. Bending analysis of laminated compositeplates was performed based on a predictor-corrector approach and the zig-zag theory by Lee andCao (1996). Alipour and Shariyat (2015) employed a zigzag-elasticity plate theory for bending andstress analysis of circular/annular sandwich plates with orthotropic composite face sheets and auxeticcores. Free vibration analysis of circular and annular composite sandwich plates with auxetic cores wasperformed by Shariyat and Alipour (2017a).

Although various studies have been presented for dynamic analysis of single layer, laminated compositeand sandwich plates, most of the existing studies were performed for plates subjected to load caseswith constant or specific amplitude. In this study dynamic response of sandwich annular plates withfunctionally graded polar orthotropic face sheets subjected to various dynamic loads are presented, asfirst time. Based on the combination of the Hinite Taylor's transform (Alipour (2016c), Shariyat and Alipour (2015, 2017b)) and the fourth-order Runge–Kutta procedure, a semi-analytical solution procedureis developed for solution of the relatively complicated second order coupled partial differentialequations. It is worth to be mentioned that modern structures are designed based on the use of compositematerials which are actually anisotropic and inhomogeneous (Peng and Li (2012) and Nie andBatra (2010)). In the presented analysis, Young's modulus in the radial and circumferential direction, shear modulus and density of each face sheet may be varied continuously in the radial direction. Thesandwich plate may be resting on viscous, elastic or viscoelastic founda-

tion. To describe more accuratelyresponse of sandwich plates, the governing differential equations of motion are derived based on theminimum total potential energy principle by using the layerwise theory. The dynamic responses ofsandwich plate are examined for various stiffness and damping coefficients of the foundation, transientloads and boundary conditions. Since no existing work has been performed on the dynamic analysis ofFG polar orthotropic sandwich plates, accuracy and efficiency of the presented analysis are verified bycomparing the obtained results with results of the three-dimensional theory of elasticity extracted fromthe ABAQUS software for some special cases. The comparisons show that there is a very good agreementbetween present results and results of the three-dimensional theory of elasticity.

2 DESCRIPTION OF THE MATERIAL PROPERTIES, DISPLACEMENT, STRAIN AND STRESS FIELDS

As shown in figure 1, a three-layer sandwich annular plate with functionally graded polar orthotropic face sheets resting on the viscoelastic substrate which is modeled as Kelvin-Voigt foundation is considered.

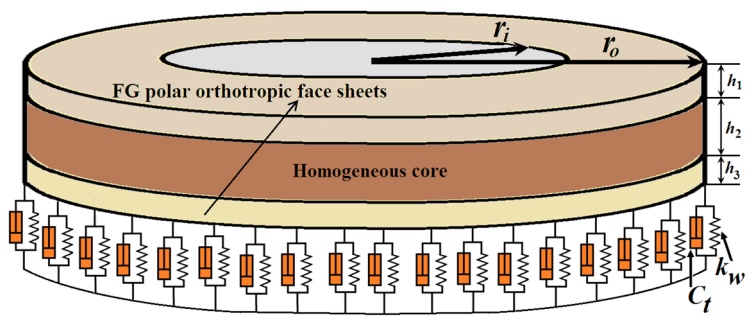

Figure 1: Schematic of the sandwich annular plate on viscoelastic substrate.

Viscoelastic substrate is modeled as a continuously distributed medium with stiffness K_w and damping coefficient C_t.

Face sheets may be fabricated from functionally graded polar orthotropic materials. Young's modulus in the radial and circumferential direction, shear modulus and density of each face sheet may be varied continuously in the radial direction according to a power-law fraction, as follows:

$$\begin{Bmatrix} E_r^{(k)}(r) \\ E_\theta^{(k)}(r) \\ G_{rz}^{(k)}(r) \end{Bmatrix} = \begin{Bmatrix} \overline{E}_r^{(k)} \\ \overline{E}_\theta^{(k)} \\ \overline{G}_{rz}^{(k)} \end{Bmatrix} \left[1 + \alpha^{(k)} \left(r - r_o \right)^{\beta^{(k)}} \right], \qquad (1)$$

$$\rho^{(k)}(r) = \overline{\rho}^{(k)} \left[1 + \gamma^{(k)} \left(r - r_o \right)^{\eta^{(k)}} \right] \qquad k = 1,3$$

$$\frac{v_{r\theta}}{E_r} = \frac{v_{\theta r}}{E_\theta} \qquad (2)$$

where $\alpha^{(k)}$, $\beta^{(k)}$, $\gamma^{(k)}$ and $\eta^{(k)}$ $(k = 1, 3)$ are inhomogeneity parameters for top (k=1) and bottom (k=3) face sheets.

The three transverse local coordinates $\xi^{(1)}$, $\xi^{(2)}$ and $\xi^{(3)}$ are represented for top, core, and bottom layers, respectively. The local coordinates are measured from the mid plane of the corresponding layer and are positive upward.

Based on the layerwise theory with the piecewise linear local components, after some manipulations and imposing the continuity conditions of the displacement components at the interfaces between face sheets and core, the displacement field of the layers may be written as:

$$\begin{aligned} u_1 &= u_0 + \left(\xi^{(1)} + \frac{h_1}{2}\right)\psi_r^{(1)} + \frac{h_2}{2}\psi_r^{(2)} \\ u_2 &= u_0 + \xi^{(2)}\psi_r^{(2)} \\ u_3 &= u_0 + \left(\xi^{(3)} - \frac{h_3}{2}\right)\psi_r^{(3)} - \frac{h_2}{2}\psi_r^{(2)}, \qquad -\frac{h_i}{2} \le \xi^{(i)} \le \frac{h_i}{2} \quad i = 1, 2, 3 \end{aligned} \tag{3}$$

where u_0 is the radial displacement component of the mid plane of the core and $\psi_r^{(i)}$ are the local rotation of the layers of the plate.

Cauchy's strain-displacement relations are:

$$\varepsilon_r = u_{,r} \quad \varepsilon_\theta = \frac{u}{r} \quad \varepsilon_{rz} = u_{,z} + w_{,r} \tag{4}$$

where the symbol "," stands for the partial derivative. Based on Hooke's generalized stress-strain law:

$$\begin{aligned} \sigma_r^{(k)} &= \frac{E_r^{(k)}(r)}{1 - v_{r\theta}^{(k)} v_{\theta r}^{(k)}}\varepsilon_r^{(k)} + \frac{v_{\theta r}^{(k)} E_r^{(k)}(r)}{1 - v_{r\theta}^{(k)} v_{\theta r}^{(k)}}\varepsilon_\theta^{(k)} \\ \sigma_\theta^{(k)} &= \frac{v_{\theta r}^{(k)} E_r^{(k)}(r)}{1 - v_{r\theta}^{(k)} v_{\theta r}^{(k)}}\varepsilon_r^{(k)} + \frac{E_\theta^{(k)}(r)}{1 - v_{r\theta}^{(k)} v_{\theta r}^{(k)}}\varepsilon_\theta^{(k)} \\ \tau_{rz}^{(k)} &= G_{rz}^{(k)}(r)\ \gamma_{rz}^{(k)} \end{aligned} \tag{5}$$

where the E, G and v symbols denote Young's modulus, shear modulus, and Poisson's ratio, respectively.

Based on Eqs.(1) to (5), the stress–displacement relations of face sheets and core may be written as:

$$\begin{aligned} \sigma_r^{(1)} &= \frac{\overline{E}_r^{(1)}\left[1 + \alpha^{(1)}\left(r - r_o\right)^{\beta^{(1)}}\right]}{1 - v_{r\theta}^{(1)} v_{\theta r}^{(1)}}\left[u_{0,r} + \frac{v_{\theta r}^{(1)}}{r}u_0 + \left(\xi^{(1)} + \frac{h_1}{2}\right)\left(\psi_{r,r}^{(1)} + \frac{v_{\theta r}^{(1)}}{r}\psi_r^{(1)}\right) + \frac{h_2}{2}\left(\psi_{r,r}^{(2)} + \frac{v_{\theta r}^{(1)}}{r}\psi_r^{(2)}\right)\right] \\ \sigma_\theta^{(1)} &= \frac{\overline{E}_\theta^{(1)}\left[1 + \alpha^{(1)}\left(r - r_o\right)^{\beta^{(1)}}\right]}{1 - v_{r\theta}^{(1)} v_{\theta r}^{(1)}}\left[v_{r\theta}^{(1)}u_{0,r} + \frac{1}{r}u_0 + \left(\xi^{(1)} + \frac{h_1}{2}\right)\left(v_{r\theta}^{(1)}\psi_{r,r}^{(1)} + \frac{1}{r}\psi_r^{(1)}\right) + \frac{h_2}{2}\left(v_{r\theta}^{(1)}\psi_{r,r}^{(2)} + \frac{1}{r}\psi_r^{(2)}\right)\right] \end{aligned} \tag{6}$$

$$\tau_{rz}^{(1)} = \bar{G}_{rz}^{(1)}\left[1+\alpha^{(1)}\left(r-r_o\right)^{\beta^{(1)}}\right]\left(\psi_r^{(1)}+w_{,r}\right)$$

$$\sigma_r^{(2)} = \frac{E^{(2)}}{1-v^{(2)2}}\left[u_{0,r}+\frac{v^{(2)}}{r}u_0+\xi^{(2)}\left(\psi_{r,r}^{(2)}+\frac{v^{(2)}}{r}\psi_r^{(2)}\right)\right]$$
$$\sigma_\theta^{(2)} = \frac{E^{(2)}}{1-v^{(2)2}}\left[v^{(2)}u_{0,r}+\frac{1}{r}u_0+\xi^{(2)}\left(v^{(2)}\psi_{r,r}^{(2)}+\frac{1}{r}\psi_r^{(2)}\right)\right]$$
$$\tau_{rz}^{(2)} = G^{(2)}\left(\psi_r^{(2)}+w_{,r}\right)$$

$$\sigma_r^{(3)} = \frac{\bar{E}_r^{(3)}\left[1+\alpha^{(3)}\left(r-r_o\right)^{\beta^{(3)}}\right]}{1-v_{r\theta}^{(3)}v_{\theta r}^{(3)}}\left[u_{0,r}+\frac{v_{\theta r}^{(3)}}{r}u_0+\left(\xi^{(3)}-\frac{h_3}{2}\right)\left(\psi_{r,r}^{(3)}+\frac{v_{\theta r}^{(3)}}{r}\psi_r^{(1)}\right)-\frac{h_2}{2}\left(\psi_{r,r}^{(2)}+\frac{v_{\theta r}^{(3)}}{r}\psi_r^{(2)}\right)\right]$$
$$\sigma_\theta^{(3)} = \frac{\bar{E}_\theta^{(3)}\left[1+\alpha^{(3)}\left(r-r_o\right)^{\beta^{(3)}}\right]}{1-v_{r\theta}^{(1)}v_{\theta r}^{(1)}}\left[v_{r\theta}^{(3)}u_{0,r}+\frac{1}{r}u_0+\left(\xi^{(3)}-\frac{h_3}{2}\right)\left(v_{r\theta}^{(3)}\psi_{r,r}^{(3)}+\frac{1}{r}\psi_r^{(3)}\right)-\frac{h_2}{2}\left(v_{r\theta}^{(3)}\psi_{r,r}^{(2)}+\frac{1}{r}\psi_r^{(2)}\right)\right]$$
$$\tau_{rz}^{(3)} = \bar{G}_{rz}^{(1)}\left[1+\alpha^{(3)}\left(r-r_o\right)^{\beta^{(3)}}\right]\left(\psi_r^{(3)}+w_{,r}\right)$$

3 THE GOVERNING EQUATIONS OF MOTION OF THE SANDWICH PLATE WITH FG POLAR ORTHOTROPIC FACE SHEETS

The governing equations of motion of the sandwich annular plate with functionally graded polar orthotropic face sheets on viscoelastic substrate are derived based on using the minimum total potential energy principle:

$$\delta\Pi = \delta U + \delta K - \delta W = 0, \tag{7}$$

where δU , δK and δW are increments of the strain energy, kinetic energy and work done by external applied loads, respectively:

$$\begin{aligned}\delta U &= \int_V \left(\sigma_r\delta\varepsilon_r+\sigma_\theta\delta\varepsilon_\theta+\tau_{rz}\delta\gamma_{rz}\right)dV\\ \delta K &= \int_V \rho\left(\ddot{u}\delta u+\ddot{w}\delta w\right)dV\\ \delta W &= \int_A P\delta w\ dA\end{aligned} \tag{8}$$

For sandwich plate subjected to transient load ($q(t)$) resting on viscoelastic substrate based on the Kelvin–Voigt model, the distributed transverse load can be defined as follows.

$$P = q(t) - K_w w(r,t) - C_t\dot{w}(r,t) \tag{9}$$

In which $q(t)$ is the external dynamic loads, K_w and C_t are the spring and damper constant of viscoelastic foundation.

Substituting Eq. (8) into Eq. (7) and by using Eqs. (3) and (6), the following five systems of second order coupled partial differential equations are resulted after some manipulations that are not included here for brevity:

$$\sum_{k=0}^{3}\left(\frac{N_r^{(k)}-N_\theta^{(k)}}{r}+N_{r,r}^{(k)}\right)=\left(I_0^{(1)}+I_0^{(2)}+I_0^{(3)}\right)\ddot{u}_0+\frac{h_1}{2}I_0^{(1)}\ddot{\psi}_r^{(1)}+\frac{h_2}{2}\left(I_0^{(1)}-I_0^{(3)}\right)\ddot{\psi}_r^{(2)}-\frac{h_3}{2}I_0^{(3)}\ddot{\psi}_r^{(3)} \tag{10}$$

$$\left(\frac{1}{r}+\frac{\partial}{\partial r}\right)\left(\frac{h_1}{2}N_r^{(1)}+M_r^{(1)}\right)-\frac{1}{r}\left(\frac{h_1}{2}N_\theta^{(1)}+M_\theta^{(1)}\right)-Q_{rz}^{(1)}=\frac{h_1}{2}I_0^{(1)}\left(\ddot{u}_0+\frac{h_2}{2}\ddot{\psi}_r^{(2)}\right)+\left(I_2^{(1)}\ddot{\psi}_r^{(1)}+\frac{h_1^2}{4}I_0^{(1)}\ddot{\psi}_r^{(1)}\right) \tag{11}$$

$$\left(\frac{1}{r}+\frac{\partial}{\partial r}\right)\left(\frac{h_2}{2}N_r^{(1)}+M_r^{(2)}-\frac{h_2}{2}N_{r,r}^{(3)}\right)-\frac{1}{r}\frac{h_2}{2}\left(N_\theta^{(1)}-N_\theta^{(3)}\right)-Q_{rz}^{(2)}=\frac{h_2}{2}I_0^{(1)}\left(\ddot{u}_0+\frac{h_1}{2}\ddot{\psi}_r^{(1)}\right)-\frac{h_2}{2}I_0^{(3)}\left(\ddot{u}_0-\frac{h_3}{2}\ddot{\psi}_r^{(3)}\right)+\left(\frac{h_2^2}{4}I_0^{(1)}+I_2^{(2)}+\frac{h_2^2}{4}I_0^{(3)}\right)\ddot{\psi}_r^{(2)} \tag{12}$$

$$\left(\frac{1}{r}+\frac{\partial}{\partial r}\right)\left(-\frac{h_3}{2}N_r^{(3)}+M_r^{(3)}\right)-Q_{rz}^{(3)}=-\frac{h_3}{2}I_0^{(3)}\left(\ddot{u}_0-\frac{h_3}{2}\ddot{\psi}_r^{(3)}\right)+\frac{h_2h_3}{4}I_0^{(3)}\ddot{\psi}_r^{(2)}+I_2^{(3)}\ddot{\psi}_r^{(3)} \tag{13}$$

$$\sum_{k=0}^{3}\left(\frac{1}{r}+\frac{\partial}{\partial r}\right)Q_r^{(k)}=q-K_w w-C_t\dot{w}+(I_0^{(1)}+I_0^{(2)}+I_0^{(3)})\ddot{w} \tag{14}$$

where the stress resultants M, N, Q and the higher-order inertias are defined as:

$$\begin{Bmatrix}N_i^{(k)}\\M_i^{(k)}\end{Bmatrix}=\int_{-\frac{h_k}{2}}^{\frac{h_k}{2}}\sigma_i^{(k)}\begin{Bmatrix}1\\\xi^{(k)}\end{Bmatrix}d\xi^{(k)},$$
$$Q_r^{(k)}=\int_{-\frac{h_k}{2}}^{\frac{h_k}{2}}\tau_{rz}^{(k)}d\xi^{(k)},\qquad k=1,2,3\ \ i=r,\theta \tag{15}$$

$$I_j^{(k)}=\int_{-\frac{h_k}{2}}^{\frac{h_k}{2}}\rho^{(k)}(r)\xi^{(k)j}d\xi^{(k)},\qquad I_j^{(k)}=\left[1+\gamma^{(k)}\left(r-r_o\right)^{\eta^{(k)}}\right]\overline{I}_j^{(k)},\qquad k=1,3$$
$$\overline{I}_j^{(i)}=\int_{-\frac{h_i}{2}}^{\frac{h_i}{2}}\overline{\rho}^{(i)}\xi^{(i)j}d\xi^{(i)}\qquad i=1,2,3\ \ j=0,2 \tag{16}$$

Based on Eq. (6), the stress resultants (Eq. (15)) may be rewritten in the following form:

$$\begin{cases} N_i^{(1)} = A_{ri}^{(1)}\left(u_{0,r} + \frac{h_1}{2}\psi_{r,r}^{(1)} + \frac{h_2}{2}\psi_{r,r}^{(2)}\right) + \frac{1}{r}A_{i\theta}^{(1)}\left(u_0 + \frac{h_1}{2}\psi_r^{(1)} + \frac{h_2}{2}\psi_r^{(2)}\right), \\ N_i^{(2)} = A_{ri}^{(2)}u_{0,r} + \frac{1}{r}A_{i\theta}^{(2)}u_0, \\ N_i^{(3)} = A_{ri}^{(3)}\left(u_{0,r} - \frac{h_3}{2}\psi_{r,r}^{(3)} - \frac{h_2}{2}\psi_{r,r}^{(2)}\right) + \frac{1}{r}A_{i\theta}^{(3)}\left(u_0 - \frac{h_3}{2}\psi_r^{(3)} - \frac{h_2}{2}\psi_r^{(2)}\right), \qquad i = r,\ \theta \end{cases} \tag{17}$$

$$M_i^{(k)} = D_{ri}^{(k)}\psi_{r,r}^{(k)} + \frac{1}{r}D_{i\theta}^{(k)}\psi_r^{(k)}, \qquad k = 1,2,3, \quad i = r,\theta \tag{18}$$

$$Q_r^{(k)} = A_{rz}^{(k)}\left(\psi_r^{(k)} + w_{,r}\right), \qquad k = 1,2,3 \tag{19}$$

where

$$\begin{Bmatrix} A_{ii}^{(k)} \\ D_{ii}^{(k)} \end{Bmatrix} = \int_{-\frac{h_k}{2}}^{\frac{h_k}{2}} \frac{E_i^{(k)}(r)}{1 - v_{r\theta}^{(k)}v_{\theta r}^{(k)}} \begin{Bmatrix} 1 \\ \xi^{(k)2} \end{Bmatrix} d\xi^{(k)}, \qquad \begin{Bmatrix} A_{r\theta}^{(k)} \\ D_{r\theta}^{(k)} \end{Bmatrix} = \int_{-\frac{h_k}{2}}^{\frac{h_k}{2}} \frac{v_{\theta r}^{(k)}E_r^{(k)}(r)}{1 - v_{r\theta}^{(k)}v_{\theta r}^{(k)}} \begin{Bmatrix} 1 \\ \xi^{(k)2} \end{Bmatrix} d\xi^{(k)},$$
$$A_{rz}^{(k)} = \int_{-\frac{h_k}{2}}^{\frac{h_k}{2}} G_{rz}^{(k)}(r)\, d\xi^{(k)}, \qquad k = 1,2,3 \quad i = r,\theta \tag{20}$$

$$\begin{Bmatrix} A_{ij}^{(k)} \\ D_{ij}^{(k)} \end{Bmatrix} = \begin{Bmatrix} \overline{A}_{ij}^{(k)} \\ \overline{D}_{ij}^{(k)} \end{Bmatrix}\left[1 + \alpha^{(k)}\left(r - r_o\right)^{\beta^{(k)}}\right],\ A_{rz}^{(k)} = \overline{A}_{rz}^{(k)}\left[1 + \alpha^{(k)}\left(r - r_o\right)^{\beta^{(k)}}\right], \quad i,j = r,\theta \ \ k = 1,3 \tag{21}$$

$$\begin{Bmatrix} \overline{A}_{ii}^{(k)} \\ \overline{D}_{ii}^{(k)} \end{Bmatrix} = \int_{-\frac{h_k}{2}}^{\frac{h_k}{2}} \frac{\overline{E}_i^{(k)}}{1 - v_{r\theta}^{(k)}v_{\theta r}^{(k)}} \begin{Bmatrix} 1 \\ \xi^{(k)2} \end{Bmatrix} d\xi^{(k)}, \quad \begin{Bmatrix} \overline{A}_{r\theta}^{(k)} \\ \overline{D}_{r\theta}^{(k)} \end{Bmatrix} = \int_{-\frac{h_k}{2}}^{\frac{h_k}{2}} \frac{v_{\theta r}^{(k)}\overline{E}_r^{(k)}}{1 - v_{r\theta}^{(k)}v_{\theta r}^{(k)}} \begin{Bmatrix} 1 \\ \xi^{(k)2} \end{Bmatrix} d\xi^{(k)},$$
$$\overline{A}_{rz}^{(k)} = \int_{-\frac{h_k}{2}}^{\frac{h_k}{2}} \overline{G}_{rz}^{(k)}\, d\xi^{(k)}, \qquad i = r,\theta \quad k = 1,3 \tag{22}$$

Based on Eqs. (15) to (22), the governing equations (10) to (14) may be rewritten as:

$$\begin{aligned} &\left[\overline{A}_{rr}^{(1)} + A_{rr}^{(2)} + \overline{A}_{rr}^{(3)} + \overline{A}_{rr}^{(1)}\alpha^{(1)}\left(r - r_o\right)^{\beta^{(1)}} + \overline{A}_{rr}^{(3)}\alpha^{(3)}\left(r - r_o\right)^{\beta^{(3)}}\right]\left(u_{0,rr} + \frac{u_{0,r}}{r}\right) \\ &-\left[\overline{A}_{\theta\theta}^{(1)} + A_{\theta\theta}^{(2)} + \overline{A}_{\theta\theta}^{(3)} + \overline{A}_{\theta\theta}^{(1)}\alpha^{(1)}\left(r - r_o\right)^{\beta^{(1)}} + \overline{A}_{\theta\theta}^{(3)}\alpha^{(3)}\left(r - r_o\right)^{\beta^{(3)}}\right]\frac{u_0}{r^2} \\ &+\frac{h_1}{2}\left[1 + \alpha^{(1)}\left(r - r_o\right)^{\beta^{(1)}}\right]\left[\overline{A}_{rr}^{(1)}\left(\psi_{r,rr}^{(1)} + \frac{\psi_{r,r}^{(1)}}{r}\right) - \overline{A}_{\theta\theta}^{(1)}\frac{\psi_r^{(1)}}{r^2}\right] \end{aligned} \tag{23}$$

$$
\begin{aligned}
&+\frac{h_2}{2}\left[\overline{A}_{rr}^{(1)}-\overline{A}_{rr}^{(3)}+\overline{A}_{rr}^{(1)}\alpha^{(1)}\left(r-r_o\right)^{\beta^{(1)}}-\overline{A}_{rr}^{(3)}\alpha^{(3)}\left(r-r_o\right)^{\beta^{(3)}}\right]\left(\psi_{r,rr}^{(2)}+\frac{\psi_{r,r}^{(2)}}{r}\right)\\
&-\frac{h_2}{2}\left[\overline{A}_{\theta\theta}^{(1)}-\overline{A}_{\theta\theta}^{(3)}+\overline{A}_{\theta\theta}^{(1)}\alpha^{(1)}\left(r-r_o\right)^{\beta^{(1)}}-\overline{A}_{\theta\theta}^{(3)}\alpha^{(3)}\left(r-r_o\right)^{\beta^{(3)}}\right]\frac{\psi_r^{(2)}}{r^2}\\
&-\frac{h_3}{2}\left[1+\alpha^{(3)}\left(r-r_o\right)^{\beta^{(3)}}\right]\left[\overline{A}_{rr}^{(3)}\left(\psi_{r,rr}^{(3)}+\frac{\psi_{r,r}^{(3)}}{r}\right)-\overline{A}_{\theta\theta}^{(3)}\frac{\psi_r^{(3)}}{r^2}\right]\\
&+\alpha^{(1)}\beta^{(1)}\left(r-r_o\right)^{\beta^{(1)}-1}\left[\left(\overline{A}_{rr}^{(1)}\frac{\partial}{\partial r}+\frac{\overline{A}_{r\theta}^{(1)}}{r}\right)\left(u_0+\frac{h_1}{2}\psi_r^{(1)}+\frac{h_2}{2}\psi_r^{(2)}\right)\right]\\
&+\alpha^{(3)}\beta^{(3)}\left(r-r_o\right)^{\beta^{(3)}-1}\left[\left(\overline{A}_{rr}^{(3)}\frac{\partial}{\partial r}+\frac{\overline{A}_{r\theta}^{(3)}}{r}\right)\left(u_0-\frac{h_3}{2}\psi_r^{(3)}-\frac{h_2}{2}\psi_r^{(2)}\right)\right]=\\
&\left(\overline{I}_0^{(1)}+\overline{I}_0^{(2)}+\overline{I}_0^{(3)}\right)\ddot{u}_0+\gamma^{(1)}\left(r-r_o\right)^{\eta^{(1)}}\overline{I}_0^{(1)}\left(\ddot{u}_0+\frac{h_1}{2}\ddot{\psi}_r^{(1)}+\frac{h_2}{2}\ddot{\psi}_r^{(2)}\right)+\frac{h_1}{2}\overline{I}_0^{(1)}\ddot{\psi}_r^{(1)}+\\
&\gamma^{(3)}\left(r-r_o\right)^{\eta^{(3)}}\overline{I}_0^{(3)}\left(\ddot{u}_0-\frac{h_2}{2}\ddot{\psi}_r^{(2)}-\frac{h_3}{2}\ddot{\psi}_r^{(3)}\right)+\frac{h_2}{2}\left(\overline{I}_0^{(1)}-\overline{I}_0^{(3)}\right)\ddot{\psi}_r^{(2)}-\frac{h_3}{2}\overline{I}_0^{(3)}\ddot{\psi}_r^{(3)}
\end{aligned}
$$

$$
\begin{aligned}
&\frac{h_1}{2}\left[1+\alpha^{(1)}\left(r-r_o\right)^{\beta^{(1)}}\right]\left[\overline{A}_{rr}^{(1)}\left(u_{0,rr}+\frac{u_{0,r}}{r}\right)-\overline{A}_{\theta\theta}^{(1)}\frac{u_0}{r^2}\right]\\
&+\left(1+\alpha^{(1)}\left(r-r_o\right)^{\beta^{(1)}}\right)\left[\left(\frac{h_1^2}{4}\overline{A}_{rr}^{(1)}+\overline{D}_{rr}^{(1)}\right)\left(\psi_{r,rr}^{(1)}+\frac{\psi_{r,r}^{(1)}}{r}\right)-\left(\frac{h_1^2}{4}\overline{A}_{\theta\theta}^{(1)}+\overline{D}_{\theta\theta}^{(1)}\right)\frac{\psi_r^{(1)}}{r^2}\right]\\
&+\frac{h_1h_2}{4}\left[1+\alpha^{(1)}\left(r-r_o\right)^{\beta^{(1)}}\right]\left[\overline{A}_{rr}^{(1)}\left(\psi_{r,rr}^{(2)}+\frac{\psi_{r,r}^{(2)}}{r}\right)-\overline{A}_{\theta\theta}^{(1)}\frac{\psi_r^{(2)}}{r^2}\right]\\
&-\overline{A}_{rz}^{(1)}\left[1+\alpha^{(1)}\left(r-r_o\right)^{\beta^{(1)}}\right]\left(\psi_r^{(1)}+w_{,r}\right)+\alpha^{(1)}\beta^{(1)}\left(r-r_o\right)^{\beta^{(1)}-1}\left(\overline{D}_{rr}^{(1)}\psi_{r,r}^{(1)}+\frac{\overline{D}_{r\theta}^{(1)}}{r}\psi_r^{(1)}\right)\\
&+\frac{h_1}{2}\alpha^{(1)}\beta^{(1)}\left(r-r_o\right)^{\beta^{(1)}-1}\left[\overline{A}_{rr}^{(1)}\left(u_{0,r}+\frac{h_1}{2}\psi_{r,r}^{(1)}+\frac{h_2}{2}\psi_{r,r}^{(2)}\right)+\frac{\overline{A}_{r\theta}^{(1)}}{r}\left(u_0+\frac{h_1}{2}\psi_r^{(1)}+\frac{h_2}{2}\psi_r^{(2)}\right)\right]\\
&=\frac{h_1}{2}\overline{I}_0^{(1)}\left(\ddot{u}_0+\frac{h_1}{2}\ddot{\psi}_r^{(1)}+\frac{h_2}{2}\ddot{\psi}_r^{(2)}\right)+\frac{h_1}{2}\overline{I}_0^{(1)}\gamma^{(1)}\left(r-r_o\right)^{\eta^{(1)}}\left(\ddot{u}_0+\frac{h_1}{2}\ddot{\psi}_r^{(1)}+\frac{h_2}{2}\ddot{\psi}_r^{(2)}\right)\\
&+\overline{I}_2^{(1)}\ddot{\psi}_r^{(1)}+\overline{I}_2^{(1)}\gamma^{(1)}\left(r-r_o\right)^{\eta^{(1)}}\ddot{\psi}_r^{(1)}
\end{aligned}
\tag{24}
$$

$$
\begin{aligned}
&\frac{h_2}{2}\left[\overline{A}_{rr}^{(1)}-\overline{A}_{rr}^{(3)}+\overline{A}_{rr}^{(1)}\alpha^{(1)}\left(r-r_o\right)^{\beta^{(1)}}-\overline{A}_{rr}^{(3)}\alpha^{(3)}\left(r-r_o\right)^{\beta^{(3)}}\right]\left(u_{0,rr}+\frac{u_{0,r}}{r}\right)\\
&-\frac{h_2}{2}\left[\overline{A}_{\theta\theta}^{(1)}-\overline{A}_{\theta\theta}^{(3)}+\overline{A}_{\theta\theta}^{(1)}\alpha^{(1)}\left(r-r_o\right)^{\beta^{(1)}}-\overline{A}_{\theta\theta}^{(3)}\alpha^{(3)}\left(r-r_o\right)^{\beta^{(3)}}\right]\frac{u_0}{r^2}\\
&+\frac{h_1h_2}{4}\overline{A}_{rr}^{(1)}\left[1+\alpha^{(1)}\left(r-r_o\right)^{\beta^{(1)}}\right]\left(\psi_{r,rr}^{(1)}+\frac{\psi_{r,r}^{(1)}}{r}\right)-\frac{h_1h_2}{4}\overline{A}_{\theta\theta}^{(1)}\left[1+\alpha^{(1)}\left(r-r_o\right)^{\beta^{(1)}}\right]\frac{\psi_r^{(1)}}{r^2}\\
&+\left[\frac{h_2^2}{4}\overline{A}_{rr}^{(1)}+D_{rr}^{(2)}+\frac{h_2^2}{4}\overline{A}_{rr}^{(3)}+\frac{h_2^2}{4}\overline{A}_{rr}^{(1)}\alpha^{(1)}\left(r-r_o\right)^{\beta^{(1)}}+\frac{h_2^2}{4}\overline{A}_{rr}^{(3)}\alpha^{(3)}\left(r-r_o\right)^{\beta^{(3)}}\right]\left(\psi_{r,rr}^{(2)}+\frac{\psi_{r,r}^{(2)}}{r}\right)
\end{aligned}
\tag{25}
$$

$$
\begin{aligned}
&-\left[\frac{h_2^2}{4}\overline{A}_{\theta\theta}^{(1)}+D_{\theta\theta}^{(2)}+\frac{h_2^2}{4}\overline{A}_{\theta\theta}^{(3)}+\frac{h_2^2}{4}\overline{A}_{\theta\theta}^{(1)}\alpha^{(1)}\left(r-r_o\right)^{\beta^{(1)}}+\frac{h_2^2}{4}\overline{A}_{\theta\theta}^{(3)}\alpha^{(3)}\left(r-r_o\right)^{\beta^{(3)}}\right]\frac{\psi_r^{(2)}}{r^2}\\
&+\frac{h_2h_3}{4}\overline{A}_{rr}^{(3)}\left[1+\alpha^{(3)}\left(r-r_o\right)^{\beta^{(3)}}\right]\left(\psi_{r,rr}^{(3)}+\frac{\psi_{r,r}^{(3)}}{r}\right)-\frac{h_2h_3}{4}\overline{A}_{\theta\theta}^{(3)}\left[1+\alpha^{(3)}\left(r-r_o\right)^{\beta^{(3)}}\right]\frac{\psi_r^{(3)}}{r^2}-A_{rz}^{(2)}\left(\psi_r^{(2)}+w_{,r}\right)\\
&+\frac{h_2}{2}\alpha^{(1)}\beta^{(1)}\left(r-r_o\right)^{\beta^{(1)}-1}\left[\overline{A}_{rr}^{(1)}\left(u_{0,r}+\frac{h_1}{2}\psi_{r,r}^{(1)}+\frac{h_2}{2}\psi_{r,r}^{(2)}\right)+\frac{\overline{A}_{r\theta}^{(1)}}{r}\left(u_0+\frac{h_1}{2}\psi_r^{(1)}+\frac{h_2}{2}\psi_r^{(2)}\right)\right]\\
&-\frac{h_2}{2}\alpha^{(3)}\beta^{(3)}\left(r-r_o\right)^{\beta^{(3)}-1}\left[\overline{A}_{rr}^{(3)}\left(u_{0,r}-\frac{h_3}{2}\psi_{r,r}^{(3)}-\frac{h_2}{2}\psi_{r,r}^{(2)}\right)+\frac{\overline{A}_{r\theta}^{(3)}}{r}\left(u_0-\frac{h_3}{2}\psi_r^{(3)}-\frac{h_2}{2}\psi_r^{(2)}\right)\right]\\
&=\frac{h_2}{2}\overline{I}_0^{(1)}\left(\ddot{u}_0+\frac{h_1}{2}\ddot{\psi}_r^{(1)}+\frac{h_2}{2}\ddot{\psi}_r^{(2)}\right)+\overline{I}_2^{(2)}\ddot{\psi}_r^{(2)}-\frac{h_2}{2}\overline{I}_0^{(3)}\left(\ddot{u}_0-\frac{h_2}{2}\ddot{\psi}_r^{(2)}-\frac{h_3}{2}\ddot{\psi}_r^{(3)}\right)+\\
&\frac{h_2}{2}\overline{I}_0^{(1)}\gamma^{(1)}\left(r-r_o\right)^{\eta^{(1)}}\left(\ddot{u}_0+\frac{h_1}{2}\ddot{\psi}_r^{(1)}+\frac{h_2}{2}\ddot{\psi}_r^{(2)}\right)-\frac{h_2}{2}\overline{I}_0^{(3)}\gamma^{(3)}\left(r-r_o\right)^{\eta^{(3)}}\left(\ddot{u}_0-\frac{h_2}{2}\ddot{\psi}_r^{(2)}-\frac{h_3}{2}\ddot{\psi}_r^{(3)}\right)
\end{aligned}
$$

$$
\begin{aligned}
&-\frac{h_3}{2}\overline{A}_{rr}^{(3)}\left[1+\alpha^{(3)}\left(r-r_o\right)^{\beta^{(3)}}\right]\left(u_{0,rr}+\frac{u_{0,r}}{r}\right)+\frac{h_3}{2}\overline{A}_{\theta\theta}^{(3)}\left[1+\alpha^{(3)}\left(r-r_o\right)^{\beta^{(3)}}\right]\frac{u_0}{r^2}\\
&+\frac{h_2h_3}{4}\left[1+\alpha^{(3)}\left(r-r_o\right)^{\beta^{(3)}}\right]\left[\overline{A}_{rr}^{(3)}\left(\psi_{r,rr}^{(2)}+\frac{\psi_{r,r}^{(2)}}{r}\right)-\overline{A}_{\theta\theta}^{(3)}\frac{\psi_r^{(2)}}{r^2}\right]\\
&+\left(\overline{D}_{rr}^{(3)}+\frac{h_3^2}{4}\overline{A}_{rr}^{(3)}\right)\left[1+\alpha^{(3)}\left(r-r_o\right)^{\beta^{(3)}}\right]\left(\psi_{r,rr}^{(3)}+\frac{\psi_{r,r}^{(3)}}{r}\right)-\left(\overline{D}_{\theta\theta}^{(3)}+\frac{h_3^2}{4}\overline{A}_{\theta\theta}^{(3)}\right)\left[1+\alpha^{(3)}\left(r-r_o\right)^{\beta^{(3)}}\right]\frac{\psi_r^{(3)}}{r^2}\\
&-\overline{A}_{rz}^{(3)}\left[1+\alpha^{(3)}\left(r-r_o\right)^{\beta^{(3)}}\right]\left(\psi_r^{(3)}+w_{,r}\right)+\alpha^{(3)}\beta^{(3)}\left(r-r_o\right)^{\beta^{(3)}-1}\left(\overline{D}_{rr}^{(3)}\psi_{r,r}^{(3)}+\frac{\overline{D}_{r\theta}^{(3)}}{r}\psi_r^{(3)}\right)\\
&-\frac{h_3}{2}\alpha^{(3)}\beta^{(3)}\left(r-r_o\right)^{\beta^{(3)}-1}\left[\overline{A}_{rr}^{(3)}\left(u_{0,r}-\frac{h_3}{2}\psi_{r,r}^{(3)}-\frac{h_2}{2}\psi_{r,r}^{(2)}\right)+\frac{\overline{A}_{r\theta}^{(3)}}{r}\left(u_0-\frac{h_3}{2}\psi_r^{(3)}-\frac{h_2}{2}\psi_r^{(2)}\right)\right]\\
&=-\frac{h_3}{2}\overline{I}_0^{(3)}\left(\ddot{u}_0-\frac{h_2}{2}\ddot{\psi}_r^{(2)}-\frac{h_3}{2}\ddot{\psi}_r^{(3)}\right)-\frac{h_3}{2}\overline{I}_0^{(3)}\gamma^{(3)}\left(r-r_o\right)^{\eta^{(3)}}\left(\ddot{u}_0-\frac{h_2}{2}\ddot{\psi}_r^{(2)}-\frac{h_3}{2}\ddot{\psi}_r^{(3)}\right)\\
&+\overline{I}_2^{(3)}\ddot{\psi}_r^{(3)}+\overline{I}_2^{(3)}\gamma^{(3)}\left(r-r_o\right)^{\eta^{(3)}}\ddot{\psi}_r^{(3)}
\end{aligned}
\tag{26}
$$

$$
\begin{aligned}
&\left[\overline{A}_{rz}^{(1)}+A_{rz}^{(2)}+\overline{A}_{rz}^{(3)}+\overline{A}_{rz}^{(1)}\alpha^{(1)}\left(r-r_o\right)^{\beta^{(1)}}+\overline{A}_{rz}^{(3)}\alpha^{(3)}\left(r-r_o\right)^{\beta^{(3)}}\right]\left(w_{,rr}+\frac{w_{,r}}{r}\right)\\
&+\overline{A}_{rz}^{(1)}\left[1+\alpha^{(1)}\left(r-r_o\right)^{\beta^{(1)}}\right]\left(\psi_{r,r}^{(1)}+\frac{\psi_r^{(1)}}{r}\right)+A_{44}^{(2)}\left(\psi_{r,r}^{(2)}+\frac{\psi_r^{(2)}}{r}\right)\\
&+\overline{A}_{rz}^{(3)}\left[1+\alpha^{(3)}\left(r-r_o\right)^{\beta^{(3)}}\right]\left(\psi_{r,r}^{(3)}+\frac{\psi_r^{(3)}}{r}\right)+\overline{A}_{rz}^{(1)}\alpha^{(1)}\beta^{(1)}\left(r-r_o\right)^{\beta^{(1)}-1}\left(\psi_r^{(1)}+w_{,r}\right)\\
&+\overline{A}_{rz}^{(3)}\alpha^{(3)}\beta^{(3)}\left(r-r_o\right)^{\beta^{(3)}-1}\left(\psi_r^{(3)}+w_{,r}\right)=-q+K_w w+C_t\dot{w}+\left(\overline{I}_0^{(1)}+\overline{I}_0^{(2)}+\overline{I}_0^{(3)}\right)\ddot{w}+\\
&\gamma^{(1)}\left(r-r_o\right)^{\eta^{(1)}}\overline{I}_0^{(1)}\ddot{w}+\gamma^{(3)}\left(r-r_o\right)^{\eta^{(3)}}\overline{I}_0^{(3)}\ddot{w}
\end{aligned}
\tag{27}
$$

For solution of the governing equations (23) to (27), various combinations of the edge conditions may be employed.

I. Clamped immovable edge:

$$\begin{cases} u_0 = 0 \\ \psi_r^{(1)} = 0 \\ \psi_r^{(2)} = 0 \\ \psi_r^{(3)} = 0 \\ w = 0 \end{cases} \tag{28}$$

II. Simply-supported movable edge:

$$\begin{cases} N_r^{(1)} + N_r^{(2)} + N_r^{(3)} = 0 \\ \frac{h_1}{2} N_r^{(1)} + M_r^{(1)} = 0 \\ \frac{h_2}{2} N_r^{(1)} + M_r^{(2)} - \frac{h_2}{2} N_r^{(3)} = 0 \\ -\frac{h_3}{2} N_r^{(3} + M_r^{(3)} = 0 \\ w = 0 \end{cases} \tag{29}$$

III. Free edge:

$$\begin{cases} N_r^{(1)} + N_r^{(2)} + N_r^{(3)} = 0 \\ \frac{h_1}{2} N_r^{(1)} + M_r^{(1)} = 0 \\ \frac{h_2}{2} N_r^{(1)} + M_r^{(2)} - \frac{h_2}{2} N_r^{(3)} = 0 \\ -\frac{h_3}{2} N_r^{(3} + M_r^{(3)} = 0 \\ Q_r^{(1)} + Q_r^{(2)} + Q_r^{(3)} = 0 \end{cases} \tag{30}$$

Also, initial conditions of the sandwich plate are:

$$\begin{aligned} &u(r,0) = \dot{u}(r,0) = 0, \\ &\psi_r^{(1)}(r,0) = \dot{\psi}_r^{(1)}(r,0) = 0, \\ &\psi_r^{(2)}(r,0) = \dot{\psi}_r^{(2)}(r,0) = 0, \\ &\psi_r^{(3)}(r,0) = \dot{\psi}_r^{(3)}(r,0) = 0, \\ &w(r,0) = \dot{w}(r,0) = 0. \end{aligned} \tag{31}$$

4 SEMI-ANALYTICAL SOLUTION FOR DYNAMIC ANALYSIS OF FG POLAR ORTHOTROPIC SANDWICH PLATE

For solution of the relatively complicated five systems of second order coupled partial differential equations, the semi-analytical solution is developed based on the finite Taylor's transform and the fourth-order Runge–Kutta procedure.

Based on Taylor's expansion, the unknown displacement functions can be expressed by the following power series:

$$\begin{Bmatrix} u_0(r,t=y\,\Delta t) \\ \dot{u}_0(r,t=y\,\Delta t) \\ \ddot{u}_0(r,t=y\,\Delta t) \end{Bmatrix} = \sum_{x=0}^{\infty} \begin{Bmatrix} U_{x,y} \\ \bar{U}_{x,y} \\ \tilde{U}_{x,y} \end{Bmatrix} \left(r-r_o\right)^x, \quad \begin{Bmatrix} \psi_r^{(1)}(r,t=y\,\Delta t) \\ \dot{\psi}_r^{(1)}(r,t=y\,\Delta t) \\ \ddot{\psi}_r^{(1)}(r,t=y\,\Delta t) \end{Bmatrix} = \sum_{x=0}^{\infty} \begin{Bmatrix} \Phi_{x,y}^{(1)} \\ \bar{\Phi}_{x,y}^{(1)} \\ \tilde{\Phi}_{x,y}^{(1)} \end{Bmatrix} \left(r-r_o\right)^x,$$
$$\begin{Bmatrix} \psi_r^{(2)}(r,t=y\,\Delta t) \\ \dot{\psi}_r^{(2)}(r,t=y\,\Delta t) \\ \ddot{\psi}_r^{(2)}(r,t=y\,\Delta t) \end{Bmatrix} = \sum_{x=0}^{\infty} \begin{Bmatrix} \Phi_{x,y}^{(2)} \\ \bar{\Phi}_{x,y}^{(2)} \\ \tilde{\Phi}_{x,y}^{(2)} \end{Bmatrix} \left(r-r_o\right)^x, \quad \begin{Bmatrix} \psi_r^{(3)}(r,t=y\,\Delta t) \\ \dot{\psi}_r^{(3)}(r,t=y\,\Delta t) \\ \ddot{\psi}_r^{(3)}(r,t=y\,\Delta t) \end{Bmatrix} = \sum_{x=0}^{\infty} \begin{Bmatrix} \Phi_{x,y}^{(3)} \\ \bar{\Phi}_{x,y}^{(3)} \\ \tilde{\Phi}_{x,y}^{(3)} \end{Bmatrix} \left(r-r_o\right)^x, \tag{32}$$
$$\begin{Bmatrix} w(r,t=y\,\Delta t) \\ \dot{w}(r,t=y\,\Delta t) \\ \ddot{w}(r,t=y\,\Delta t) \end{Bmatrix} = \sum_{x=0}^{\infty} \begin{Bmatrix} W_{x,y} \\ \bar{W}_{x,y} \\ \tilde{W}_{x,y} \end{Bmatrix} \left(r-r_o\right)^x$$

where ΔT is the time step, y is the time step counter and $U_{x,y}$, $\bar{U}_{x,y}$, $\tilde{U}_{x,y}$, $\Phi_{x,y}^{(1)}$, $\bar{\Phi}_{x,y}^{(1)}$, $\tilde{\Phi}_{x,y}^{(1)}$, $\Phi_{x,y}^{(2)}$, $\bar{\Phi}_{x,y}^{(2)}$, $\tilde{\Phi}_{x,y}^{(2)}$, $\Phi_{x,y}^{(3)}$, $\bar{\Phi}_{x,y}^{(3)}$, $\tilde{\Phi}_{x,y}^{(3)}$, $W_{x,y}$, $\bar{W}_{x,y}$ and $\tilde{W}_{x,y}$ are the coefficients of series in each time step.

On the other hands, Taylor transform of the functions $1/r$ and $1/r^2$ may be expressed by the following power series whose center is located at r=ro.

$$\frac{1}{r} = -\sum_{s=0}^{\infty}\left(-\frac{1}{r_o}\right)^{s+1}\left(r-r_o\right)^s, \quad \frac{1}{r^2} = \sum_{s=0}^{\infty}(s+1)\left(-\frac{1}{r_o}\right)^{s+2}\left(r-r_o\right)^s \tag{33}$$

In practical applications, the transformed form of functions must be expressed by means of finite series.

The transformed form of the governing equations may be obtained by substituting Eqs. (32) and (33) into the governing Eqs. (23) to (27) and performing some manipulations.

$$\begin{aligned}
&\sum_{x=0}^{X}\left[\left(\bar{A}_{rr}^{(1)}+A_{rr}^{(2)}+\bar{A}_{rr}^{(3)}\right)\left[(x+2)(x+1)U_{x+2,y}-\sum_{s=0}^{x}\chi^{s+1}(x-s+1)U_{x-s+1,y}\right]\right.\\
&\bar{A}_{rr}^{(1)}\alpha^{(1)}\left[\left(x-\beta^{(1)}+2\right)\left(x-\beta^{(1)}+1\right)U_{x-\beta^{(1)}+2,y}-\sum_{s=0}^{x-\beta^{(1)}}\chi^{s+1}\left(x-\beta^{(1)}-s+1\right)U_{x-\beta^{(1)}-s+1,y}\right]+\\
&\bar{A}_{rr}^{(3)}\alpha^{(3)}\left[\left(x-\beta^{(3)}+2\right)\left(x-\beta^{(3)}+1\right)U_{x-\beta^{(3)}+2,y}-\sum_{s=0}^{x-\beta^{(3)}}\chi^{s+1}\left(x-\beta^{(3)}-s+1\right)U_{x-\beta^{(3)}-s+1,y}\right]+\\
&-\left(\bar{A}_{\theta\theta}^{(1)}+A_{\theta\theta}^{(2)}+\bar{A}_{\theta\theta}^{(3)}\right)\sum_{s=0}^{x}(s+1)\chi^{s+2}U_{x-s,y}-\bar{A}_{\theta\theta}^{(1)}\alpha^{(1)}\sum_{s=0}^{x-\beta^{(1)}}(s+1)\chi^{s+2}U_{x-\beta^{(1)}-s,y}\\
&-\bar{A}_{\theta\theta}^{(3)}\alpha^{(3)}\sum_{s=0}^{x-\beta^{(3)}}(s+1)\chi^{s+2}U_{x-\beta^{(3)}-s,y}+\frac{h_1}{2}\bar{A}_{rr}^{(1)}\left[(x+2)(x+1)\Phi_{x+2,y}^{(1)}-\sum_{s=0}^{x}\chi^{s+1}(x-s+1)\Phi_{x-s+1,y}^{(1)}\right]\\
&\left.+\frac{h_1}{2}\bar{A}_{rr}^{(1)}\alpha^{(1)}\left[\left(x-\beta^{(1)}+2\right)\left(x-\beta^{(1)}+1\right)\Phi_{x-\beta^{(1)}+2,y}^{(1)}-\sum_{s=0}^{x-\beta^{(1)}}\chi^{s+1}\left(x-\beta^{(1)}-s+1\right)\Phi_{x-\beta^{(1)}-s+1,y}^{(1)}\right]\right.
\end{aligned} \tag{34}$$

$$
\begin{aligned}
&-\frac{h_1}{2}\overline{A}^{(1)}_{\theta\theta}\sum_{s=0}^{x}(s+1)\chi^{s+2}\Phi^{(1)}_{x-s,y}-\frac{h_1}{2}\overline{A}^{(1)}_{\theta\theta}\alpha^{(1)}\sum_{s=0}^{x-\beta^{(1)}}(s+1)\chi^{s+2}\Phi^{(1)}_{x-\beta^{(1)}-s,y}\\
&+\frac{h_2}{2}\Big(\overline{A}^{(1)}_{rr}-\overline{A}^{(3)}_{rr}\Big)\left[(x+2)(x+1)\Phi^{(2)}_{x+2,y}-\sum_{s=0}^{x}\chi^{s+1}(x-s+1)\Phi^{(2)}_{x-s+1,y}\right]\\
&+\frac{h_2}{2}\overline{A}^{(1)}_{rr}\alpha^{(1)}\left[\Big(x-\beta^{(1)}+2\Big)\Big(x-\beta^{(1)}+1\Big)\Phi^{(2)}_{x-\beta^{(1)}+2,y}-\sum_{s=0}^{x-\beta^{(1)}}\chi^{s+1}\Big(x-\beta^{(1)}-s+1\Big)\Phi^{(2)}_{x-\beta^{(1)}-s+1,y}\right]\\
&-\frac{h_2}{2}\overline{A}^{(3)}_{rr}\alpha^{(3)}\left[\Big(x-\beta^{(3)}+2\Big)\Big(x-\beta^{(3)}+1\Big)\Phi^{(2)}_{x-\beta^{(3)}+2,y}-\sum_{s=0}^{x-\beta^{(3)}}\chi^{s+1}\Big(x-\beta^{(3)}-s+1\Big)\Phi^{(2)}_{x-\beta^{(3)}-s+1,y}\right]\\
&-\frac{h_2}{2}\Big(\overline{A}^{(1)}_{\theta\theta}-\overline{A}^{(3)}_{\theta\theta}\Big)\sum_{s=0}^{x}(s+1)\chi^{s+2}\Phi^{(2)}_{x-s,y}-\frac{h_2}{2}\overline{A}^{(1)}_{\theta\theta}\alpha^{(1)}\sum_{s=0}^{x-\beta^{(1)}}(s+1)\chi^{s+2}\Phi^{(2)}_{x-\beta^{(1)}-s,y}\\
&+\frac{h_2}{2}\overline{A}^{(3)}_{\theta\theta}\alpha^{(3)}\sum_{s=0}^{x-\beta^{(3)}}(s+1)\chi^{s+2}\Phi^{(2)}_{x-\beta^{(3)}-s,y}-\frac{h_3}{2}\overline{A}^{(3)}_{rr}\left[(x+2)(x+1)\Phi^{(3)}_{x+2,y}-\sum_{s=0}^{x}\chi^{s+1}(x-s+1)\Phi^{(3)}_{x-s+1,y}\right]\\
&-\frac{h_3}{2}\overline{A}^{(3)}_{rr}\alpha^{(3)}\left[\Big(x-\beta^{(3)}+2\Big)\Big(x-\beta^{(3)}+1\Big)\Phi^{(3)}_{x-\beta^{(3)}+2,y}-\sum_{s=0}^{x-\beta^{(3)}}\chi^{s+1}\Big(x-\beta^{(3)}-s+1\Big)\Phi^{(3)}_{x-\beta^{(3)}-s+1,y}\right]\\
&+\frac{h_3}{2}\overline{A}^{(3)}_{\theta\theta}\sum_{s=0}^{x}(s+1)\chi^{s+2}\Phi^{(3)}_{x-s,y}+\alpha^{(1)}\beta^{(1)}\overline{A}^{(1)}_{rr}\Big(x-\beta^{(1)}+2\Big)\left(U_{x-\beta^{(1)}+2,y}+\frac{h_1}{2}\Phi^{(1)}_{x-\beta^{(1)}+2}+\frac{h_2}{2}\Phi^{(2)}_{x-\beta^{(1)}+2,y}\right)\\
&+\frac{h_3}{2}\overline{A}^{(3)}_{\theta\theta}\alpha^{(3)}\sum_{s=0}^{x-\beta^{(3)}}(s+1)\chi^{s+2}\Phi^{(3)}_{x-\beta^{(3)}-s,y}-\alpha^{(1)}\beta^{(1)}\overline{A}^{(1)}_{r\theta}\sum_{s=0}^{x-\beta^{(1)}+1}\chi^{s+1}\left(U_{x-s-\beta^{(1)}+1}+\frac{h_1}{2}\Phi^{(1)}_{x-s-\beta^{(1)}+1,y}+\frac{h_2}{2}\Phi^{(2)}_{x-s-\beta^{(1)}+1,y}\right)\\
&+\alpha^{(3)}\beta^{(3)}\overline{A}^{(3)}_{rr}\Big(x-\beta^{(3)}+2\Big)\left(U_{x-\beta^{(3)}+2,y}-\frac{h_3}{2}\Phi^{(3)}_{x-\beta^{(3)}+2,y}-\frac{h_2}{2}\Phi^{(2)}_{x-\beta^{(3)}+2,y}\right)\\
&-\alpha^{(3)}\beta^{(3)}\overline{A}^{(3)}_{r\theta}\sum_{s=0}^{x-\beta^{(3)}+1}\chi^{s+1}\left(U_{x-s-\beta^{(3)}+1,y}-\frac{h_3}{2}\Phi^{(3)}_{x-s-\beta^{(3)}+1,y}-\frac{h_2}{2}\Phi^{(2)}_{x-s-\beta^{(3)}+1,y}\right)\\
&-\Big(\overline{I}^{(1)}_0+\overline{I}^{(2)}_0+\overline{I}^{(3)}_0\Big)\tilde{U}_{x,y}-\gamma^{(1)}\overline{I}^{(1)}_0\tilde{U}_{x-\eta^{(1)},y}-\gamma^{(2)}\overline{I}^{(2)}_0\tilde{U}_{x-\eta^{(2)},y}-\gamma^{(3)}\overline{I}^{(3)}_0\tilde{U}_{x-\eta^{(3)},y}\\
&-\frac{h_1}{2}\overline{I}^{(1)}_0\tilde{\Phi}^{(1)}_{x,y}-\frac{h_2}{2}\Big(\overline{I}^{(1)}_0-\overline{I}^{(3)}_0\Big)\tilde{\Phi}^{(2)}_{x,y}+\frac{h_3}{2}\overline{I}^{(3)}_0\tilde{\Phi}^{(3)}_{x,y}-\gamma^{(1)}\overline{I}^{(1)}_0\left(\frac{h_1}{2}\tilde{\Phi}^{(1)}_{x-\eta^{(1)},y}+\frac{h_2}{2}\tilde{\Phi}^{(2)}_{x-\eta^{(1)},y}\right)\\
&+\gamma^{(3)}\overline{I}^{(3)}_0\left(\frac{h_2}{2}\tilde{\Phi}^{(2)}_{x-\eta^{(3)},y}+\frac{h_3}{2}\tilde{\Phi}^{(3)}_{x-\eta^{(3)},y}\right)\Bigg](r-r_o)^x=0
\end{aligned}
$$

$$
\begin{aligned}
&\sum_{x=0}^{X}\Bigg\{\frac{h_1}{2}\overline{A}^{(1)}_{rr}\left[(x+2)(x+1)U_{x+2,y}-\sum_{s=0}^{x}\chi^{s+1}(x-s+1)U_{x-s+1,y}\right]-\frac{h_1}{2}\overline{A}^{(1)}_{\theta\theta}\sum_{s=0}^{x}(s+1)\chi^{s+2}U_{x-s,y}\\
&+\frac{h_1}{2}\overline{A}^{(1)}_{rr}\alpha^{(1)}\left[(x-\beta^{(1)}+2)(x-\beta^{(1)}+1)U_{x-\beta^{(1)}+2,y}-\sum_{s=0}^{x-\beta^{(1)}}\chi^{s+1}(x-\beta^{(1)}-s+1)U_{x-\beta^{(1)}-s+1,y}\right]\\
&-\frac{h_1}{2}\overline{A}^{(1)}_{\theta\theta}\alpha^{(1)}\sum_{s=0}^{x-\beta^{(1)}}(s+1)\chi^{s+2}U_{x-\beta^{(1)}-s,y}+\left(\frac{h_1^2}{4}\overline{A}^{(1)}_{rr}+\overline{D}^{(1)}_{rr}\right)\left[(x+2)(x+1)\Phi^{(1)}_{x+2,y}-\sum_{s=0}^{x}\chi^{s+1}(x-s+1)\Phi^{(1)}_{x-s+1,y}\right]\\
&+\left(\frac{h_1^2}{4}\overline{A}^{(1)}_{rr}+\overline{D}^{(1)}_{rr}\right)\alpha^{(1)}\left[(x-\beta^{(1)}+2)(x-\beta^{(1)}+1)\Phi^{(1)}_{x-\beta^{(1)}+2,y}-\sum_{s=0}^{x-\beta^{(1)}}\chi^{s+1}(x-\beta^{(1)}-s+1)\Phi^{(1)}_{x-\beta^{(1)}-s+1,y}\right]\\
&-\left(\frac{h_1^2}{4}\overline{A}^{(1)}_{\theta\theta}+\overline{D}^{(1)}_{\theta\theta}\right)\sum_{s=0}^{x}(s+1)\chi^{s+2}\Phi^{(1)}_{x-s,y}-\left(\frac{h_1^2}{4}\overline{A}^{(1)}_{\theta\theta}+\overline{D}^{(1)}_{\theta\theta}\right)\alpha^{(1)}\sum_{s=0}^{x-\beta^{(1)}}(s+1)\chi^{s+2}\Phi^{(1)}_{x-\beta^{(1)}-s,y}\\
&+\frac{h_1h_2}{4}\overline{A}^{(1)}_{rr}\left[(x+2)(x+1)\Phi^{(2)}_{x+2,y}-\sum_{s=0}^{x}\chi^{s+1}(x-s+1)\Phi^{(2)}_{x-s+1,y}\right]-\alpha^{(1)}\beta^{(1)}\overline{D}^{(1)}_{r\theta}\sum_{s=0}^{x-\beta^{(1)}+1}\chi^{s+1}\Phi^{(1)}_{x-s-\beta^{(1)}+1,y}\\
&+\frac{h_1h_2}{4}\alpha^{(1)}\overline{A}^{(1)}_{rr}\left[\Big(x-\beta^{(1)}+2\Big)\Big(x-\beta^{(1)}+1\Big)\Phi^{(2)}_{x-\beta^{(1)}+2,y}-\sum_{s=0}^{x-\beta^{(1)}}\chi^{s+1}\Big(x-\beta^{(1)}-s+1\Big)\Phi^{(2)}_{x-\beta^{(1)}-s+1,y}\right]
\end{aligned}
\tag{35}
$$

$$
\begin{aligned}
&-\frac{h_1h_2}{4}\,\overline{A}^{(1)}_{\theta\theta}\sum_{s=0}^{x}(s+1)\chi^{s+2}\Phi^{(2)}_{x-s,y}-\frac{h_1h_2}{4}\,\alpha^{(1)}\overline{A}^{(1)}_{\theta\theta}\sum_{s=0}^{x-\beta^{(1)}}(s+1)\chi^{s+2}\Phi^{(2)}_{x-\beta^{(1)}-s,y}\\
&-\overline{A}^{(1)}_{rz}\Big[\Phi^{(1)}_{x,y}+(x+1)W_{x+1,y}\Big]-\overline{A}^{(1)}_{rz}\alpha^{(1)}\Big[\Phi^{(1)}_{x-\beta^{(1)},y}+\Big(x-\beta^{(1)}+1\Big)W_{x-\beta^{(1)}+1,y}\Big]+\alpha^{(1)}\beta^{(1)}\overline{D}^{(1)}_{rr}\Big(x-\beta^{(1)}+2\Big)\Phi^{(1)}_{x-\beta^{(1)}+2,y}\\
&+\frac{h_1}{2}\alpha^{(1)}\beta^{(1)}\overline{A}^{(1)}_{rr}\Big(x-\beta^{(1)}+2\Big)\Bigg(U_{x-\beta^{(1)}+2,y}+\frac{h_1}{2}\Phi^{(1)}_{x-\beta^{(1)}+2,y}+\frac{h_2}{2}\Phi^{(2)}_{x-\beta^{(1)}+2,y}\Bigg)\\
&-\frac{h_1}{2}\alpha^{(1)}\beta^{(1)}\overline{A}^{(1)}_{r\theta}\sum_{s=0}^{x-\beta^{(1)}+1}\chi^{s+1}\Bigg(U_{x-s-\beta^{(1)}+1,y}+\frac{h_1}{2}\Phi^{(1)}_{x-s-\beta^{(1)}+1,y}+\frac{h_2}{2}\Phi^{(2)}_{x-s-\beta^{(1)}+1,y}\Bigg)\\
&-\frac{h_1}{2}\overline{I}^{(1)}_{0}\Bigg(\tilde{U}_{x,y}+\frac{h_1}{2}\tilde{\Phi}^{(1)}_{x,y}+\frac{h_2}{2}\tilde{\Phi}^{(2)}_{x,y}\Bigg)-\frac{h_1}{2}\overline{I}^{(1)}_{0}\gamma^{(1)}\Bigg(\tilde{U}_{x-\eta^{(1)},y}+\frac{h_1}{2}\tilde{\Phi}^{(1)}_{x-\eta^{(1)},y}+\frac{h_2}{2}\tilde{\Phi}^{(2)}_{x-\eta^{(1)},y}\Bigg)\\
&-\overline{I}^{(1)}_{2}\tilde{\Phi}^{(1)}_{x,y}-\overline{I}^{(1)}_{2}\gamma^{(1)}\tilde{\Phi}^{(1)}_{x-\eta^{(1)},y}\Bigg\}(r-r_0)^x=0
\end{aligned}
$$

$$
\begin{aligned}
&\sum_{x=0}^{X}\Bigg\{\frac{h_2}{2}\Big(\overline{A}^{(1)}_{rr}-\overline{A}^{(3)}_{rr}\Big)\Bigg[(x+2)(x+1)U_{x+2,y}-\sum_{s=0}^{x}\chi^{s+1}(x-s+1)U_{x-s+1,y}\Bigg]\\
&+\frac{h_2}{2}\overline{A}^{(1)}_{rr}\alpha^{(1)}\Bigg[\Big(x-\beta^{(1)}+2\Big)\Big(x-\beta^{(1)}+1\Big)U_{x-\beta^{(1)}+2,y}-\sum_{s=0}^{x-\beta^{(1)}}\chi^{s+1}\Big(x-\beta^{(1)}-s+1\Big)U_{x-\beta^{(1)}-s+1,y}\Bigg]\\
&-\frac{h_2}{2}\overline{A}^{(3)}_{rr}\alpha^{(3)}\Bigg[\Big(x-\beta^{(3)}+2\Big)\Big(x-\beta^{(3)}+1\Big)U_{x-\beta^{(3)}+2,y}-\sum_{s=0}^{x-\beta^{(3)}}\chi^{s+1}\Big(x-\beta^{(3)}-s+1\Big))U_{x-\beta^{(3)}-s+1,y}\Bigg]\\
&-\frac{h_2}{2}\Big(\overline{A}^{(1)}_{\theta\theta}-\overline{A}^{(3)}_{\theta\theta}\Big)\sum_{s=0}^{x}(s+1)\chi^{s+2}U_{x-s,y}-\frac{h_2}{2}\overline{A}^{(1)}_{\theta\theta}\alpha^{(1)}\sum_{s=0}^{x-\beta^{(1)}}(s+1)\chi^{s+2}U_{x-\beta^{(1)}-s,y}\\
&+\frac{h_2}{2}\overline{A}^{(3)}_{\theta\theta}\alpha^{(3)}\sum_{s=0}^{x-\beta^{(1)}}(s+1)\chi^{s+2}U_{x-\beta^{(3)}-s,y}+\frac{h_1h_2}{4}\overline{A}^{(1)}_{rr}\Bigg[(x+2)(x+1)\Phi^{(1)}_{x+2,y}-\sum_{s=0}^{x}\chi^{s+1}(x-s+1)\Phi^{(1)}_{x-s+1,y}\Bigg]\\
&+\frac{h_1h_2}{4}\overline{A}^{(1)}_{rr}\alpha^{(1)}\Bigg[\Big(x-\beta^{(1)}+2\Big)\Big(x-\beta^{(1)}+1\Big)\Phi^{(1)}_{x-\beta^{(1)}+2,y}-\sum_{s=0}^{x-\beta^{(1)}}\chi^{s+1}\Big(x-\beta^{(1)}-s+1\Big)\Phi^{(1)}_{x-\beta^{(1)}-s+1,y}\Bigg]\\
&-\frac{h_1h_2}{4}\overline{A}^{(1)}_{\theta\theta}\sum_{s=0}^{x}(s+1)\chi^{s+2}\Phi^{(1)}_{x-s,y}-\frac{h_1h_2}{4}\overline{A}^{(1)}_{\theta\theta}\alpha^{(1)}\sum_{s=0}^{x-\beta^{(1)}}(s+1)\chi^{s+2}\Phi^{(1)}_{x-\beta^{(1)}-s,y}\\
&+\Bigg(\frac{h_2^2}{4}\overline{A}^{(1)}_{rr}+D^{(2)}_{rr}+\frac{h_2^2}{4}\overline{A}^{(3)}_{rr}\Bigg)\Bigg[(x+2)(x+1)\Phi^{(2)}_{x+2,y}-\sum_{s=0}^{x}\chi^{s+1}(x-s+1)\Phi^{(2)}_{x-s+1,y}\Bigg]\\
&+\frac{h_2^2}{4}\overline{A}^{(1)}_{rr}\alpha^{(1)}\Bigg[\Big(x-\beta^{(1)}+2\Big)\Big(x-\beta^{(1)}+1\Big)\Phi^{(2)}_{x-\beta^{(1)}+2,y}-\sum_{s=0}^{x-\beta^{(1)}}\chi^{s+1}\Big(x-\beta^{(1)}-s+1\Big)\Phi^{(2)}_{x-\beta^{(1)}-s+1,y}\Bigg]\\
&+\frac{h_2^2}{4}\overline{A}^{(3)}_{rr}\alpha^{(3)}\Bigg[\Big(x-\beta^{(3)}+2\Big)\Big(x-\beta^{(3)}+1\Big)\Phi^{(2)}_{x-\beta^{(3)}+2,y}-\sum_{s=0}^{x-\beta^{(3)}}\chi^{s+1}\Big(x-\beta^{(3)}-s+1\Big)\Phi^{(2)}_{x-\beta^{(3)}-s+1,y}\Bigg]\\
&-\Bigg(\frac{h_2^2}{4}\overline{A}^{(1)}_{\theta\theta}+D^{(2)}_{\theta\theta}+\frac{h_2^2}{4}\overline{A}^{(3)}_{\theta\theta}\Bigg)\sum_{s=0}^{x}(s+1)\chi^{s+2}\Phi^{(2)}_{x-s,y}-\frac{h_2^2}{4}\overline{A}^{(1)}_{\theta\theta}\alpha^{(1)}\sum_{s=0}^{x-\beta^{(1)}}(s+1)\chi^{s+2}\Phi^{(2)}_{x-\beta^{(1)}-s,y}\\
&-\frac{h_2^2}{4}\overline{A}^{(3)}_{\theta\theta}\alpha^{(3)}\sum_{s=0}^{x-\beta^{(3)}}(s+1)\chi^{s+2}\Phi^{(2)}_{x-\beta^{(3)}-s,y}+\frac{h_2h_3}{4}\overline{A}^{(3)}_{rr}\Bigg[(x+2)(x+1)\Phi^{(3)}_{x+2,y}-\sum_{s=0}^{x}\chi^{s+1}\Big(x-s+1\Big)\Phi^{(3)}_{x-s+1,y}\Bigg]\\
&+\frac{h_2h_3}{4}\overline{A}^{(3)}_{rr}\alpha^{(3)}\Bigg[\Big(x-\beta^{(3)}+2\Big)\Big(x-\beta^{(3)}+1\Big)\Phi^{(3)}_{x-\beta^{(3)}+2,y}-\sum_{s=0}^{x-\beta^{(3)}}\chi^{s+1}\Big(x-\beta^{(3)}-s+1\Big)\Phi^{(3)}_{x-\beta^{(3)}-s+1,y}\Bigg]\\
&-\frac{h_2h_3}{4}\overline{A}^{(3)}_{\theta\theta}\sum_{s=0}^{x}(s+1)\chi^{s+2}\Phi^{(3)}_{x-s,y}-\frac{h_2h_3}{4}\overline{A}^{(3)}_{\theta\theta}\alpha^{(3)}\sum_{s=0}^{x-\beta^{(3)}}(s+1)\chi^{s+2}\Phi^{(3)}_{x-\beta^{(3)}-s,y}-A^{(2)}_{rz}\Big[\Phi^{(2)}_{x}+(x+1)W_{x+1,y}\Big]\\
&+\frac{h_2}{2}\alpha^{(1)}\beta^{(1)}\overline{A}^{(1)}_{rr}\Big(x-\beta^{(1)}+2\Big)\Bigg(U_{x-\beta^{(1)}+2,y}+\frac{h_1}{2}\Phi^{(1)}_{x-\beta^{(1)}+2,y}+\frac{h_2}{2}\Phi^{(2)}_{x-\beta^{(1)}+2,y}\Bigg)
\end{aligned}
\tag{36}
$$

$$
\begin{aligned}
&-\frac{h_2}{2}\alpha^{(1)}\beta^{(1)}\overline{A}^{(1)}_{r\theta}\sum_{s=0}^{\infty}\chi^{s+1}\left(U_{x-s-\beta^{(1)}+1,y}+\frac{h_1}{2}\Phi^{(1)}_{x-s-\beta^{(1)}+1,y}+\frac{h_2}{2}\Phi^{(2)}_{x-s-\beta^{(1)}+1,y}\right)\\
&-\frac{h_2}{2}\alpha^{(3)}\beta^{(3)}\overline{A}^{(3)}_{rr}\left(x-\beta^{(3)}+2\right)\left(U_{x-\beta^{(3)}+2,y}-\frac{h_3}{2}\Phi^{(3)}_{x-\beta^{(3)}+2,y}-\frac{h_2}{2}\Phi^{(2)}_{x-\beta^{(3)}+2,y}\right)\\
&+\frac{h_2}{2}\alpha^{(3)}\beta^{(3)}\overline{A}^{(3)}_{r\theta}\sum_{s=0}^{\infty}\chi^{s+1}\left(U_{x-s-\beta^{(3)}+1,y}-\frac{h_3}{2}\Phi^{(3)}_{x-s-\beta^{(3)}+1,y}-\frac{h_2}{2}\Phi^{(2)}_{x-s-\beta^{(3)}+1,y}\right)\\
&-\frac{h_2}{2}\overline{I}^{(1)}_0\left(\tilde{U}_{x,y}+\frac{h_1}{2}\tilde{\Phi}^{(1)}_{x,y}+\frac{h_2}{2}\tilde{\Phi}^{(2)}_{x,y}\right)-\overline{I}^{(2)}_2\tilde{\Phi}^{(2)}_{x,y}+\frac{h_2}{2}\overline{I}^{(3)}_0\left(\tilde{U}_{x,y}-\frac{h_2}{2}\tilde{\Phi}^{(2)}_{x,y}-\frac{h_3}{2}\tilde{\Phi}^{(3)}_{x,y}\right)\\
&-\frac{h_2}{2}\overline{I}^{(1)}_0\gamma^{(1)}\left(\tilde{U}_{x-\eta^{(1)},y}+\frac{h_1}{2}\tilde{\Phi}^{(1)}_{x-\eta^{(1)},y}+\frac{h_2}{2}\tilde{\Phi}^{(2)}_{x-\eta^{(1)},y}\right)-\overline{I}^{(2)}_2\gamma^{(2)}\tilde{\Phi}^{(2)}_{x-\eta^{(2)},y}\\
&+\frac{h_2}{2}\overline{I}^{(3)}_0\gamma^{(3)}\left(\tilde{U}_{x-\eta^{(3)},y}-\frac{h_2}{2}\tilde{\Phi}^{(2)}_{x-\eta^{(3)},y}-\frac{h_3}{2}\tilde{\Phi}^{(3)}_{x-\eta^{(3)},y}\right)\Bigg\}(r-r_0)^x=0
\end{aligned}
$$

$$
\begin{aligned}
&\sum_{x=0}^{X}\Bigg\{-\frac{h_3}{2}\overline{A}^{(3)}_{rr}\left[(x+2)(x+1)U_{x+2,y}-\sum_{s=0}^{x}\chi^{s+1}(x-s+1)U_{x-s+1,y}\right]\\
&-\frac{h_3}{2}\overline{A}^{(3)}_{rr}\alpha^{(3)}\left[\left(x-\beta^{(3)}+2\right)\left(x-\beta^{(3)}+1\right)U_{x-\beta^{(3)}+2,y}-\sum_{s=0}^{x-\beta^{(3)}}\chi^{s+1}\left(x-\beta^{(3)}-s+1\right)U_{x-\beta^{(3)}-s+1,y}\right]\\
&+\frac{h_3}{2}\overline{A}^{(3)}_{\theta\theta}\sum_{s=0}^{x}(s+1)\chi^{s+2}U_{x-s,y}+\frac{h_3}{2}\overline{A}^{(3)}_{\theta\theta}\alpha^{(3)}\sum_{s=0}^{x-\beta^{(1)}}(s+1)\chi^{s+2}U_{x-\beta^{(3)}-s,y}\\
&+\frac{h_2h_3}{4}\overline{A}^{(3)}_{rr}\left[(x+2)(x+1)\Phi^{(2)}_{x+2,y}-\sum_{s=0}^{x}\chi^{s+1}(x-s+1)\Phi^{(2)}_{x-s+1,y}\right]\\
&+\frac{h_2h_3}{4}\overline{A}^{(3)}_{rr}\alpha^{(3)}\left[\left(x-\beta^{(3)}+2\right)\left(x-\beta^{(3)}+1\right)\Phi^{(2)}_{x-\beta^{(3)}+2,y}-\sum_{s=0}^{x-\beta^{(3)}}\chi^{s+1}\left(x-\beta^{(3)}-s+1\right)\Phi^{(2)}_{x-\beta^{(3)}-s+1,y}\right]\\
&-\frac{h_2h_3}{4}\overline{A}^{(3)}_{\theta\theta}\sum_{s=0}^{x}(s+1)\chi^{s+2}\Phi^{(2)}_{x-s,y}-\frac{h_2h_3}{4}\overline{A}^{(3)}_{\theta\theta}\alpha^{(3)}\sum_{s=0}^{x-\beta^{(3)}}(s+1)\chi^{s+2}\Phi^{(2)}_{x-\beta^{(3)}-s,y}\\
&+\left(\overline{D}^{(3)}_{rr}+\frac{h_3^2}{4}\overline{A}^{(3)}_{rr}\right)\left[(x+2)(x+1)\Phi^{(3)}_{x+2,y}-\sum_{s=0}^{x}\chi^{s+1}(x-s+1)\Phi^{(3)}_{x-s+1,y}\right]\\
&+\left(\overline{D}^{(3)}_{rr}+\frac{h_3^2}{4}\overline{A}^{(3)}_{rr}\right)\alpha^{(3)}\left[\left(x-\beta^{(3)}+2\right)\left(x-\beta^{(3)}+1\right)\Phi^{(3)}_{x-\beta^{(3)}+2,y}-\sum_{s=0}^{x-\beta^{(3)}}\chi^{s+1}\left(x-\beta^{(3)}-s+1\right)\Phi^{(3)}_{x-\beta^{(3)}-s+1,y}\right]\\
&-\left(\overline{D}^{(3)}_{\theta\theta}+\frac{h_3^2}{4}\overline{A}^{(3)}_{\theta\theta}\right)\sum_{s=0}^{x}(s+1)\chi^{s+2}\Phi^{(3)}_{x-s,y}-\left(\overline{D}^{(3)}_{\theta\theta}+\frac{h_3^2}{4}\overline{A}^{(3)}_{\theta\theta}\right)\alpha^{(3)}\sum_{s=0}^{x-\beta^{(3)}}(s+1)\chi^{s+2}\Phi^{(3)}_{x-\beta^{(3)}-s,y}\\
&-\overline{A}^{(3)}_{rz}\left(\Phi^{(3)}_{x}+(x+1)W_{x+1}\right)-\overline{A}^{(3)}_{rz}\alpha^{(3)}\left[\Phi^{(3)}_{x-\beta^{(3)}}+\left(x-\beta^{(3)}+1\right)W_{x-\beta^{(3)}+1}\right]\\
&+\alpha^{(3)}\beta^{(3)}\overline{D}^{(3)}_{rr}\left(x-\beta^{(3)}+2\right)\Phi^{(3)}_{x-\beta^{(3)}+2,y}-\alpha^{(3)}\beta^{(3)}\overline{D}^{(3)}_{r\theta}\sum_{s=0}^{\infty}\chi^{s+1}\Phi^{(3)}_{x-s-\beta^{(3)}+1,y}\\
&-\frac{h_3}{2}\alpha^{(3)}\beta^{(3)}\overline{A}^{(3)}_{rr}(x-\beta^{(3)}+2)\left(U_{x-\beta^{(3)}+2,y}-\frac{h_3}{2}\Phi^{(3)}_{x-\beta^{(3)}+2,y}-\frac{h_2}{2}\Phi^{(2)}_{x-\beta^{(3)}+2,y}\right)\\
&+\frac{h_3}{2}\alpha^{(3)}\beta^{(3)}\overline{A}^{(3)}_{r\theta}\sum_{s=0}^{\infty}\chi^{s+1}\left(U_{x-s-\beta^{(3)}+1,y}-\frac{h_3}{2}\Phi^{(3)}_{x-s-\beta^{(3)}+1,y}-\frac{h_2}{2}\Phi^{(2)}_{x-s-\beta^{(3)}+1,y}\right)-\overline{I}^{(3)}_2\gamma^{(3)}\tilde{\Phi}^{(3)}_{x-\eta^{(3)},y}-\overline{I}^{(3)}_2\tilde{\Phi}^{(3)}_{x,y}\\
&+\frac{h_3}{2}\overline{I}^{(3)}_0\left(\tilde{U}_{x,y}-\frac{h_3}{2}\tilde{\Phi}^{(3)}_{x,y}-\frac{h_2}{2}\tilde{\Phi}^{(2)}_{x,y}\right)+\frac{h_3}{2}\overline{I}^{(3)}_0\gamma^{(3)}\left(\tilde{U}_{x,y}-\frac{h_3}{2}\tilde{\Phi}^{(3)}_{x-\eta^{(3)},y}-\frac{h_2}{2}\tilde{\Phi}^{(2)}_{x-\eta^{(3)},y}\right)\Bigg\}(r-r_o)^x=0
\end{aligned}
\tag{37}
$$

$$
\begin{aligned}
&\sum_{x=0}^{X}\Bigg\{\Big(\overline{A}_{rz}^{(1)}+A_{rz}^{(2)}+\overline{A}_{rz}^{(3)}\Big)\Bigg[(x+2)(x+1)W_{x+2,y}-\sum_{s=0}^{x}\chi^{s+1}(x-s+1)W_{x-s+1,y}\Bigg]\\
&+\overline{A}_{rz}^{(1)}\alpha^{(1)}\Bigg[\Big(x-\beta^{(1)}+2\Big)\Big(x-\beta^{(1)}+1\Big)W_{x-\beta^{(1)}+2,y}-\sum_{s=0}^{x-\beta^{(1)}}\chi^{s+1}\Big(x-\beta^{(1)}-s+1\Big)W_{x-\beta^{(1)}-s+1,y}\Bigg]\\
&+\overline{A}_{rz}^{(3)}\alpha^{(3)}\Bigg[\Big(x-\beta^{(3)}+2\Big)\Big(x-\beta^{(3)}+1\Big)W_{x-\beta^{(3)}+2,y}-\sum_{s=0}^{x-\beta^{(3)}}\chi^{s+1}\Big(x-\beta^{(3)}-s+1\Big)W_{x-\beta^{(3)}-s+1,y}\Bigg]\\
&+\overline{A}_{rz}^{(1)}(x+1)\Phi_{x+1,y}^{(1)}+\overline{A}_{rz}^{(1)}\alpha^{(1)}(x-\beta^{(1)}+1)\Phi_{x-\beta^{(1)}+1,y}^{(1)}-\overline{A}_{rz}^{(1)}\sum_{s=0}^{\infty}\chi^{s+1}\Phi_{x-s,y}^{(1)}-\overline{A}_{rz}^{(1)}\alpha^{(1)}\sum_{s=0}^{\infty}\chi^{s+1}\Phi_{x-s-\beta^{(1)},y}^{(1)}\\
&+A_{44}^{(2)}\Bigg[(x+1)\Phi_{x+1,y}^{(2)}-\sum_{s=0}^{\infty}\chi^{s+1}\Phi_{x-s,y}^{(2)}\Bigg]+\overline{A}_{rz}^{(3)}(x+1)\Phi_{x+1,y}^{(3)}+\overline{A}_{rz}^{(3)}\alpha^{(3)}\Big(x-\beta^{(3)}+1\Big)\Phi_{x-\beta^{(3)}+1,y}^{(3)}\\
&-\overline{A}_{rz}^{(3)}\sum_{s=0}^{\infty}\chi^{s+1}\Phi_{x-s,y}^{(3)}-\overline{A}_{rz}^{(3)}\alpha^{(3)}\sum_{s=0}^{\infty}\chi^{s+1}\Phi_{x-\beta^{(3)}-s,y}^{(3)}+\overline{A}_{rz}^{(1)}\alpha^{(1)}\beta^{(1)}\Phi_{x-\beta^{(1)}+1,y}^{(1)}+q\delta(x)-K_{w}W_{x,y}-C_{t}\overline{W}_{x,y}\\
&+\overline{A}_{rz}^{(1)}\alpha^{(1)}\beta^{(1)}(x-\beta^{(1)}+2)W_{x-\beta^{(1)}+2,y}+\overline{A}_{rz}^{(3)}\alpha^{(3)}\beta^{(3)}\Phi_{x-\beta^{(3)}+1,y}^{(3)}+\overline{A}_{rz}^{(3)}\alpha^{(3)}\beta^{(3)}\Big(x-\beta^{(3)}+2\Big)W_{x-\beta^{(3)}+2,y}\\
&-\Big(\overline{I}_{0}^{(1)}+\overline{I}_{0}^{(2)}+\overline{I}_{0}^{(3)}\Big)\tilde{W}_{x,y}-\gamma^{(1)}\overline{I}_{0}^{(1)}\tilde{W}_{x-\eta^{(1)},y}-\gamma^{(2)}\overline{I}_{0}^{(2)}\tilde{W}_{x-\eta^{(2)},y}-\gamma^{(3)}\overline{I}_{0}^{(3)}\tilde{W}_{x-\eta^{(3)},y}\Bigg\}(r-r_{o})^{x}=0
\end{aligned}
\tag{38}
$$

Where $\delta(x)$ is Kronecker's delta function.

The transformed forms of the various boundary conditions at the inner (r=r_i) and outer (r=r_o) edges can be obtained by substituting Eq. (32) into the Eqs. (28-30).

$$
\begin{aligned}
u=0 &\Rightarrow \sum_{x=0}^{X}U_{x,y}(r-r_{o})^{x}=0\\
\psi_{r}^{(1)}=0 &\Rightarrow \sum_{x=0}^{X}\Phi_{x,y}^{(1)}(r-r_{o})^{x}=0,\\
\psi_{r}^{(2)}=0 &\Rightarrow \sum_{x=0}^{X}\Phi_{x,y}^{(2)}(r-r_{o})^{x}=0,\\
\psi_{r}^{(3)}=0 &\Rightarrow \sum_{x=0}^{X}\Phi_{x,y}^{(3)}(r-r_{o})^{x}=0,\\
w=0 &\Rightarrow \sum_{x=0}^{X}W_{x,y}(r-r_{o})^{x}=0
\end{aligned}
\tag{39}
$$

$$
\begin{aligned}
&N_{r}^{(1)}+N_{r}^{(2)}+N_{r}^{(3)}=0\ \Rightarrow\\
&\sum_{x=0}^{X}\Bigg\{\Big[1+\alpha^{(1)}\big(r-r_{o}\big)^{\beta^{(1)}}\Big]\Bigg[\overline{A}_{rr}^{(1)}(x+1)\Bigg(U_{x+1,y}+\frac{h_{1}}{2}\Phi_{x+1,y}^{(1)}+\frac{h_{2}}{2}\Phi_{x+1,y}^{(2)}\Bigg)-\frac{\overline{A}_{r\theta}^{(1)}}{r}\Bigg(U_{x,y}+\frac{h_{1}}{2}\Phi_{x,y}^{(1)}+\frac{h_{2}}{2}\Phi_{x,y}^{(2)}\Bigg)\Bigg]+\\
&\quad\Big[1+\alpha^{(3)}\big(r-r_{o}\big)^{\beta^{(3)}}\Big]\Bigg[\overline{A}_{rr}^{(3)}(x+1)\Bigg(U_{x+1,y}-\frac{h_{2}}{2}\Phi_{x+1,y}^{(2)}-\frac{h_{3}}{2}\Phi_{x+1,y}^{(3)}\Bigg)-\frac{\overline{A}_{r\theta}^{(3)}}{r}\Bigg(U_{x,y}-\frac{h_{2}}{2}\Phi_{x,y}^{(2)}-\frac{h_{3}}{2}\Phi_{x,y}^{(3)}\Bigg)\Bigg]\\
&\quad A_{rr}^{(2)}(x+1)U_{x+1,y}-\overline{A}_{r\theta}^{(2)}\frac{U_{x,y}}{r}\Bigg\}\big(r-r_{o}\big)^{x}=0
\end{aligned}
\tag{40}
$$

$$
\begin{aligned}
&\frac{h_{1}}{2}N_{r}^{(1)}+M_{r}^{(1)}=0\Rightarrow\\
&\quad\sum_{x=0}^{X}\Bigg\{\frac{h_{1}}{2}\Big[1+\alpha^{(1)}\big(r-r_{o}\big)^{\beta^{(1)}}\Big]\Bigg[\overline{A}_{rr}^{(1)}(x+1)\Bigg(U_{x+1,y}+\frac{h_{1}}{2}\Phi_{x+1,y}^{(1)}+\frac{h_{2}}{2}\Phi_{x+1,y}^{(2)}\Bigg)-\frac{\overline{A}_{r\theta}^{(1)}}{r}\Bigg(U_{x,y}+\frac{h_{1}}{2}\Phi_{x,y}^{(1)}+\frac{h_{2}}{2}\Phi_{x,y}^{(2)}\Bigg)\Bigg]
\end{aligned}
$$

$$+\left[1+\alpha^{(1)}\left(r-r_o\right)^{\beta^{(1)}}\right]\left(\bar{D}^{(1)}_{rr}\psi^{(1)}_{r,r}+\frac{1}{r}\bar{D}^{(1)}_{r\theta}\psi^{(1)}_{r}\right)\Bigg\}\left(r-r_o\right)^{x}=0$$

$$\frac{h_2}{2}N^{(1)}_{r}+M^{(2)}_{r}-\frac{h_2}{2}N^{(3)}_{r}=0\Rightarrow$$

$$\sum_{x=0}^{X}\Bigg\{\frac{h_2}{2}\left[1+\alpha^{(1)}\left(r-r_o\right)^{\beta^{(1)}}\right]\left[\bar{A}^{(1)}_{rr}(x+1)\left(U_{x+1,y}+\frac{h_1}{2}\Phi^{(1)}_{x+1,y}+\frac{h_2}{2}\Phi^{(2)}_{x+1,y}\right)-\frac{\bar{A}^{(1)}_{r\theta}}{r}\left(U_{x,y}+\frac{h_1}{2}\Phi^{(1)}_{x,y}+\frac{h_2}{2}\Phi^{(2)}_{x,y}\right)\right]$$

$$-\frac{h_2}{2}\left[1+\alpha^{(3)}\left(r-r_o\right)^{\beta^{(3)}}\right]\left[\bar{A}^{(3)}_{rr}(x+1)\left(U_{x+1,y}-\frac{h_2}{2}\Phi^{(2)}_{x+1,y}-\frac{h_3}{2}\Phi^{(3)}_{x+1,y}\right)-\frac{\bar{A}^{(3)}_{r\theta}}{r}\left(U_{x,y}-\frac{h_2}{2}\Phi^{(2)}_{x,y}-\frac{h_3}{2}\Phi^{(3)}_{x,y}\right)\right]$$

$$D^{(2)}_{rr}\psi^{(2)}_{r,r}+\frac{1}{r}D^{(2)}_{r\theta}\psi^{(2)}_{r}\Bigg\}\left(r-r_o\right)^{x}=0$$

$$-\frac{h_3}{2}N^{(3}_{r}+M^{(3)}_{r}=0\Rightarrow$$

$$\sum_{x=0}^{X}\Bigg\{-\frac{h_3}{2}\left[1+\alpha^{(3)}\left(r-r_o\right)^{\beta^{(3)}}\right]\left[\bar{A}^{(3)}_{rr}(x+1)\left(U_{x+1,y}-\frac{h_2}{2}\Phi^{(2)}_{x+1,y}-\frac{h_3}{2}\Phi^{(3)}_{x+1,y}\right)-\frac{\bar{A}^{(3)}_{r\theta}}{r}\left(U_{x,y}-\frac{h_2}{2}\Phi^{(2)}_{x,y}-\frac{h_3}{2}\Phi^{(3)}_{x,y}\right)\right]$$

$$+\left[1+\alpha^{(3)}\left(r-r_o\right)^{\beta^{(3)}}\right]\left(\bar{D}^{(3)}_{rr}\psi^{(3)}_{r,r}+\frac{1}{r}\bar{D}^{(3)}_{r\theta}\psi^{(3)}_{r}\right)\Bigg\}\left(r-r_o\right)^{x}=0$$

$$Q^{(1)}_{r}+Q^{(2)}_{r}+Q^{(3)}_{r}=0\Rightarrow$$

$$\sum_{x=0}^{X}\Bigg\{\bar{A}^{(1)}_{rz}\left[1+\alpha^{(1)}\left(r-r_o\right)^{\beta^{(1)}}\right]\left[\Phi^{(1)}_{x,y}+(x+1)W_{x+1,y}\right]+A^{(2)}_{rz}\left[\Phi^{(2)}_{x,y}+(x+1)W_{x+1,y}\right]+$$

$$\bar{A}^{(3)}_{rz}\left[1+\alpha^{(3)}\left(r-r_o\right)^{\beta^{(3)}}\right]\left[\Phi^{(3)}_{x,y}+(x+1)W_{x+1,y}\right]\Bigg\}\left(r-r_o\right)^{x}=0$$

The resulting governing differential equations can be solved in terms of time by the fourth-order Runge-Kutta method, numerically.

The unknown displacement, velocity and acceleration parameters can be expressed as following vectors:

$$\begin{aligned}F(r,t)&=\left\langle u(r,t),\ \psi^{(1)}_{r}(r,t),\ \psi^{(2)}_{r}(r,t),\ \psi^{(3)}_{r}(r,t),\ w(r,t)\right\rangle\\ \dot{F}(r,t)&=\left\langle \dot{u}(r,t),\ \dot{\psi}^{(1)}_{r}(r,t),\ \dot{\psi}^{(2)}_{r}(r,t),\ \dot{\psi}^{(3)}_{r}(r,t),\ \dot{w}(r,t)\right\rangle\\ \ddot{F}(r,t)&=\left\langle \ddot{u}(r,t),\ \ddot{\psi}^{(1)}_{r}(r,t),\ \ddot{\psi}^{(2)}_{r}(r,t),\ \ddot{\psi}^{(3)}_{r}(r,t),\ \ddot{w}(r,t)\right\rangle\end{aligned}\tag{41}$$

Also, the transformed forms of the unknown parameters may be expressed as following vectors:

$$\begin{aligned}F_{x,y}&=\left\langle U_{x,y},\ \Phi^{(1)}_{x,y},\ \Phi^{(2)}_{x,y},\ \Phi^{(3)}_{x,y},\ W_{x,y}\right\rangle\\ \bar{F}_{x,y}&=\left\langle \bar{U}_{x,y},\ \bar{\Phi}^{(1)}_{x,y},\ \bar{\Phi}^{(2)}_{x,y},\ \bar{\Phi}^{(3)}_{x,y},\ \bar{W}_{x,y}\right\rangle\\ \tilde{F}_{x,y}&=\left\langle \tilde{U}_{x,y},\ \tilde{\Phi}^{(1)}_{x,y},\ \tilde{\Phi}^{(2)}_{x,y},\ \tilde{\Phi}^{(3)}_{x,y},\ \tilde{W}_{x,y}\right\rangle\end{aligned}\tag{42}$$

Based on the fourth-order Runge-Kutta method, when the acceleration and velocity parameters at $t=y\Delta t$ are known as $\bar{F}_{x,y}$ and $\tilde{F}_{x,y}$ the displacement parameters at $t=y\Delta t$ and $t=\left(y+1\right)\Delta t$ are known as $F_{x,y}$ and $F_{x,y+1}$, the acceleration and velocity parameters at $t=\left(y+1\right)\Delta t$ can be found by using the following formulations:

$$\tilde{F}_{x,y+1}=\frac{4}{\Delta t^2}\left(F_{x,y+1}-F_{x,y}-\Delta t\,\bar{F}_{x,y}-\frac{1}{4}\Delta t^2\tilde{F}_{x,y}\right)\tag{43}$$

$$\bar{F}_{x,y+1} = \bar{F}_{x,y} + \frac{\Delta t}{2}\left(\tilde{F}_{x,y} - \tilde{F}_{x,y+1}\right) \tag{44}$$

By using Eqs. (31) and (32), the initial conditions can be obtained as following transformed forms:

$$\begin{aligned} U_{x,0} &= \bar{U}_{x,0} = 0, \\ \Phi^{(1)}_{x,0} &= \bar{\Phi}^{(1)}_{x,0} = 0, \\ \Phi^{(2)}_{x,0} &= \bar{\Phi}^{(2)}_{x,0} = 0, \\ \Phi^{(3)}_{x,0} &= \bar{\Phi}^{(3)}_{x,0} = 0, \\ W_{x,0} &= \bar{W}_{x,0} = 0, \end{aligned} \tag{45}$$

The unknown functions can be obtained by using the transformed forms of the governing equations Eqs. (34)-(38), boundary conditions Eqs. (39, 40) and initial conditions Eq. (45) and the relations between the acceleration, velocity and displacement parameters Eqs. (43) and (44). From the Eqs. (39) and (40), five equations for each edge must be applied (based on the edge condition at the inner and outer edges).

The unknown functions may be obtained according to the following steps.

I. Initial values of the acceleration parameters $\left(\tilde{F}_{x,0}\right)$ are determined based on the Eqs. (34)-(38) and Eq. (45).

II. From Eqs. (42) and (43), the acceleration and velocity parameters at the end of each time step $\left(\tilde{F}_{x,y} \text{ and } \bar{F}_{x,y},\ y = 1,2,3,...\right)$ may be expressed based on the obtained parameters at the previous step $\left(F_{x,y-1},\ \tilde{F}_{x,y-1} \text{ and } \bar{F}_{x,y-1},\quad y = 1,2,3,...\right)$ and unknown displacement parameters at the end of each time step $\left(F_{x,y},\quad y = 1,2,3,...\right)$.

III. The displacements parameters at the end of each time step $\left(F_{x,y}\right)$ are determined based on the obtained results of the acceleration and velocity parameters from step (II), Eqs. (34)-(38) and the edge conditions (Eqs. (39, 40)) corresponding to the end of each time step.

IV. Repeating steps (II) and (III) till the final time instant is reached $\left(t = y\ \Delta T\right)$.

5 RESULTS AND DISCUSSIONS

In this section, effects of the viscoelastic foundation on the transient response of the functionally graded polar orthotropic sandwich annular plates are investigated. The presented results cover various dynamic loads, edge conditions and foundation parameters. Dynamic responses of the sandwich structures are extracted for various dynamic loads as $q = \hat{q}\, f(t)$, in which $\hat{q}$ is the maximum amplitude and $f(t)$ is an arbitrary unit time-dependency function.

In the presented results, the following dynamic load cases are examined (as shown in figure2):

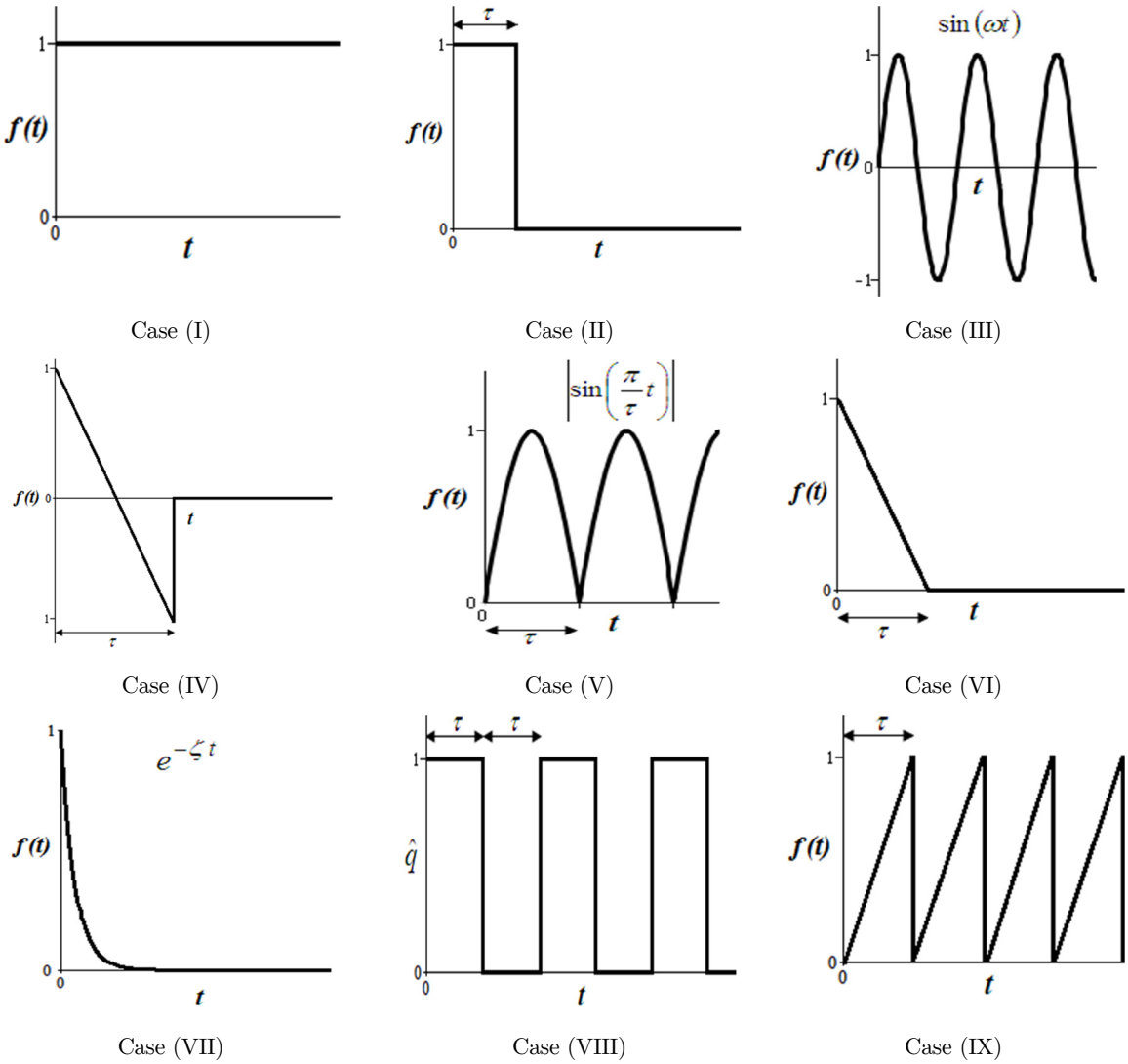

Figure 2: The various kinds of dynamic loads in numerical examples.

Case I) Step loading: $f(t) = 1$

Case II) Pulse loading: $$f(t) = \begin{cases} 1 & \text{for} \quad 0 \le t \le \tau \\ 0 & \text{for} \quad \tau \le t \end{cases}$$

Case III) Sinusoidal loading: $f(t) = \sin(\omega t)$

Case IV)N-shaped pulse loading: $$f(t) = \begin{cases} 1 - \dfrac{2t}{\tau} & \text{for} \quad 0 \le t \le \tau \\ 0 & \text{for} \quad \tau \le t \end{cases}$$

Case V) Sinusoidal loading acting in the same direction: $$f(t) = \left| \sin\left(\frac{\pi}{\tau} t \right) \right|$$

Case VI) A triangular-shaped pulse loading: $f(t)=\begin{cases}1-\dfrac{t}{\tau} & \text{for} \quad 0\le t\le\tau \\ 0 & \text{for} \quad \tau\le t\end{cases}$

Case VII) Exponential loading: $f(t)=e^{-\zeta t}$

Case VIII) Repeated rectangular-shaped loading:

$$f(t)=\begin{cases}1 & \text{for} \quad 2i\tau\le t\le(2i+1)\tau \\ 0 & \text{for} \quad (2i+1)\tau\le t\le 2(i+1)\tau\end{cases} \qquad i=0,1,2,...$$

Case IX)Repeated triangular-shaped loading:

$$f(t)=\frac{t-i\tau}{\tau} \qquad \text{for} \quad 2i\tau\le t\le(2i+1)\tau \qquad i=0,1,2,...$$

Sandwich plates under dynamic loads with the maximum amplitude of $\hat{q}=1\text{MPa}$ are considered throughout the examples. Also, the following geometric information and material properties for the homogenous core are chosen.

$$r_i=0.2, \quad r_o=1, \quad h_1=0.1, \quad h_2=0.2, \; h_3=0.1, \; E^{(2)}=20 \text{ GPa},$$
$$\rho^{(2)}=950\big/g \;\; \text{N/m}^3, \quad v^{(2)}=0.25, \quad g=9.81 \;\; m/s^2$$

5.1 Transient Response of Heterogeneous Sandwich Plate

In this study, dynamic response of sandwich circular plate with functionally graded orthotropic face sheets are presented as first time and no available results may be found in literature to demonstrate the efficiency and accuracy of the obtained results. For this reason, as a verification example, the obtained results are verified by comparison with finite element results for some special cases. The finite element results are extracted from the ABAQUS software based on the three dimensional theory of elasticity. In this example, sandwich plate with heterogeneous face sheets and asymmetric layups is considered and effects of the damping coefficient on the transient response of heterogeneous sandwich plate are examined. The face sheets have the same stiffness in the radial and circumferential directions as:

$$\begin{cases}E_r^{(1)}(r)=E_\theta^{(1)}(r)=310\Big[1-\big(r-r_o\big)^2\Big]\text{GPa} \\ \rho^{(1)}(r)=1613\Big[1-\big(r-r_o\big)^2\Big]\Big/g \;\; \text{N/m}^3 \\ v_{r\theta}^{(1)}=v_{\theta r}^{(1)}=0.26\end{cases}, \quad \begin{cases}E_r^{(3)}(r)=E_\theta^{(3)}(r)=310\big[1+0.5\big(r-r_o\big)\big]\text{ GPa} \\ \rho^{(3)}(r)=1613\big[1+0.5\big(r-r_o\big)\big]\big/g \;\; \text{N/m}^3 \\ v_{r\theta}^{(3)}=v_{\theta r}^{(3)}=0.23\end{cases},$$

$$G^{(k)}(r)=\frac{E_r^{(k)}(r)}{2(1+v_{r\theta}^{(k)})}$$

Dynamic responses of the sandwich annular plate with clamped-free boundary condition (clamped inner edge and free outer edge) are shown in figures 3-5 for the load cases (I), (II) and (III), respectively. In these figures, time variations of the lateral deflection at the outer edge of

sandwich plate are plotted for k_w=0 and various values of the damping coefficients of viscoelastic foundation C_t. Also, the obtained results are compared with results of ABAQUS finite element software when there is no foundation (k_w= C_t =0). It can be seen that there is an excellent agreement between present results based on the analytical solution (AS) and results of ABAQUS software which are extracted based on the finite element method (FEM). It is shown that when the damping coefficient increases, vibration amplitude becomes smaller, as expected due to the dissipation of system energy. Figure 3 shows that the plate oscillates about the static deflection (W_{Static}) and for C_t =0 (when there is no damping in the foundation) the maximum deflection will be as: $W_{Dynamic\text{-}Maximum}$=2 W_{Static}. Also for plate subjected to step loading rested on viscous foundation, as time goes on, the dynamic lateral deflection tends to static response. Time variations of the lateral deflection of the plate under load case (II) are plotted in figure 4 for time duration $\tau = 0.5$ and 1.5 ms. In this type of loading, the dynamic responses of the plate are separated into two stages as follow:

a) Forced vibration (plate under the step loading) $t < \tau$

The plate oscillates about the static deflection of the plate under the step loading.

b) Free vibration (the load is removed) $t > \tau$

The plate oscillates about the zero.

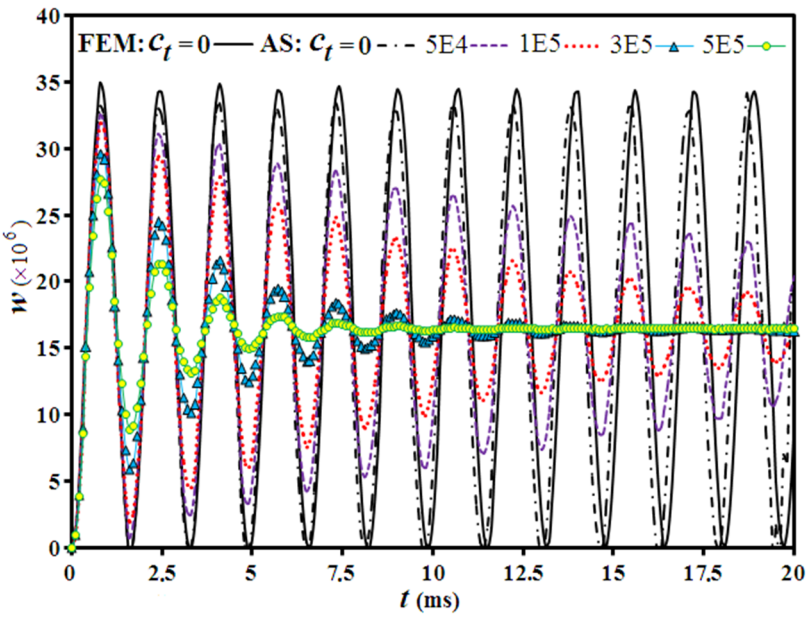

Figure 3: Dynamic response of clamped-free sandwich annular plate subjected to an abrupt uniformly distributed transverse load (case (I)).

As expected for plate subjected to a pulse loading rested on viscous foundation, the amplitude decreases and approaches zero as time increases.

Dynamic responses of sandwich plate under sinusoidal loading (case (III)) are illustrated in figure 5 for various frequency of the harmonic excitation (ω). Value of the parameter ω is chosen as a ratio of the fundamental natural frequency ($\Omega = 3892.5$) of the plate. As it is expected for plate

under sinusoidal load with harmonic excitation $\omega = \Omega$, the oscillation amplitude becomes unbounded in undamped system (figure 5(a)). However, there is not an obvious increase in the amplitude of oscillation when the damping coefficient increases up to 3E5 or 8E5.

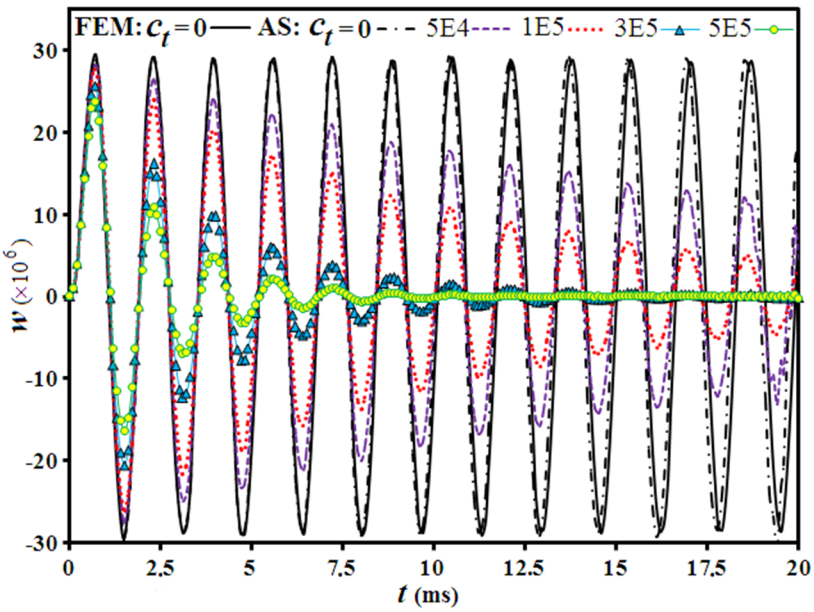

(a)

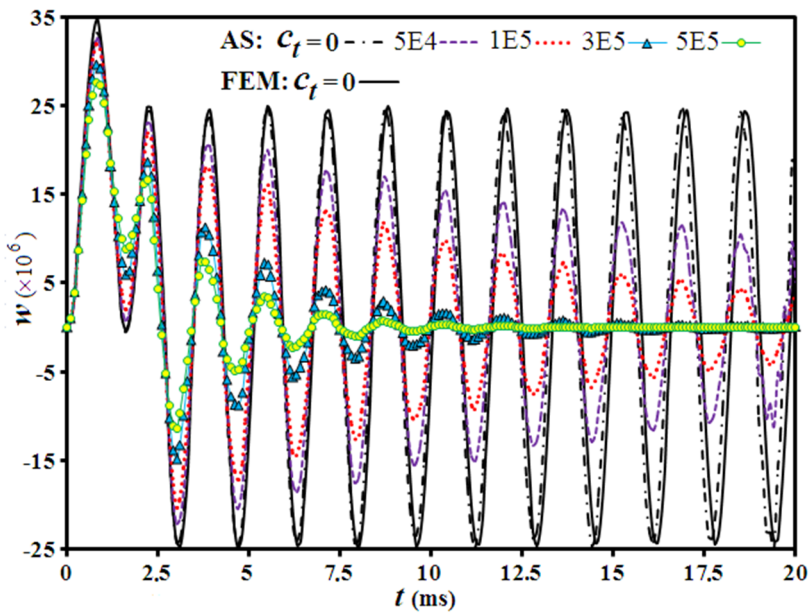

(b)

Figure 4: Dynamic response of clamped-free sandwich annular plate subjected to an abruptly-imposed uniform transverse load (Case (II)) with time duration: (a) $t_0 = 0.5$ ms and (b) $t_0 = 2$ ms.

It can be seen from figures 5(b), (c) and (d) that for excitation frequencies $\omega = \Omega / 4, \Omega / 6,$ and $\Omega / 8$, influence of other vibration modes are superimposed on the main response in undamped system. On the other hands the dynamic response of plates resting on the viscous foundation (damped system) is smoother and the local oscillations are eliminated. It is observed that the peak deflection slightly decreases as excitation frequency decreases. These figures also show that increasing the damping coefficient of viscous foundation reduces the amplitude and frequency of vibration.

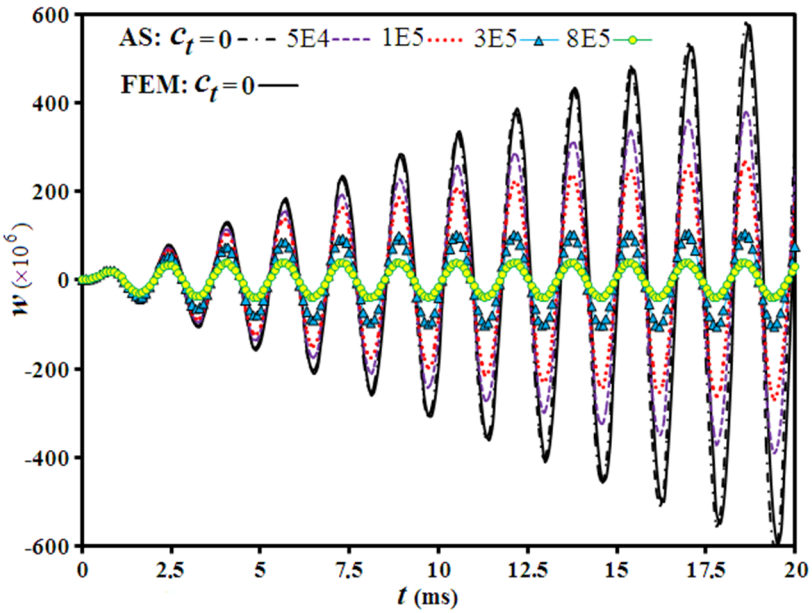

(a)

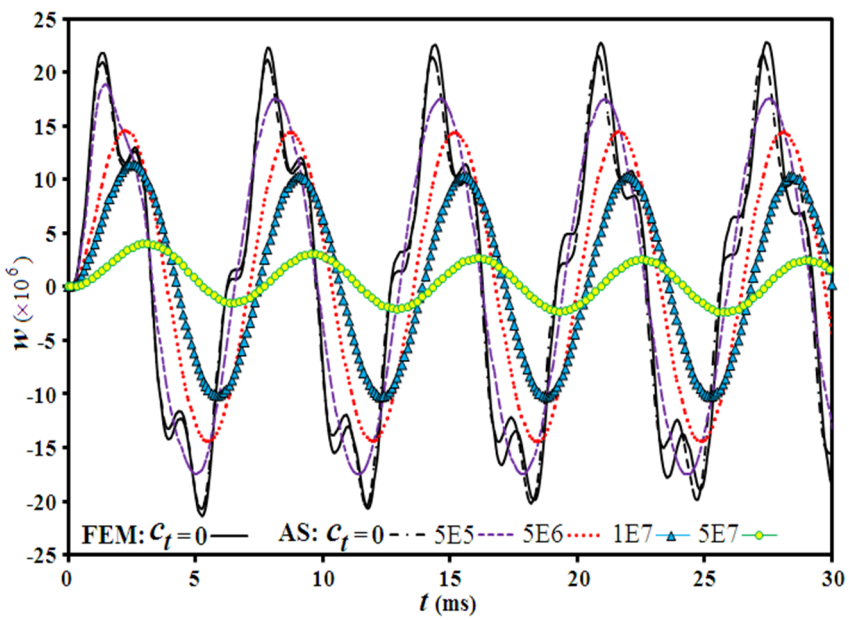

(b)

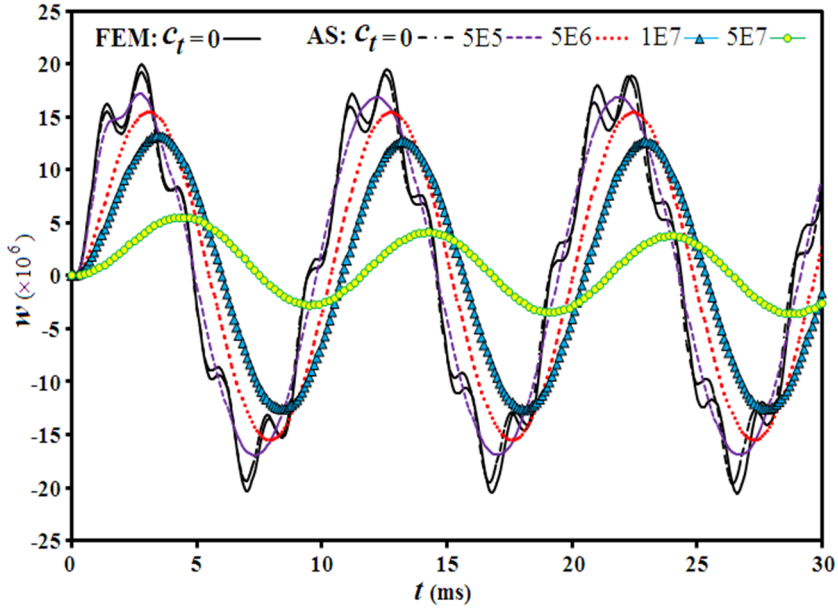

(c)

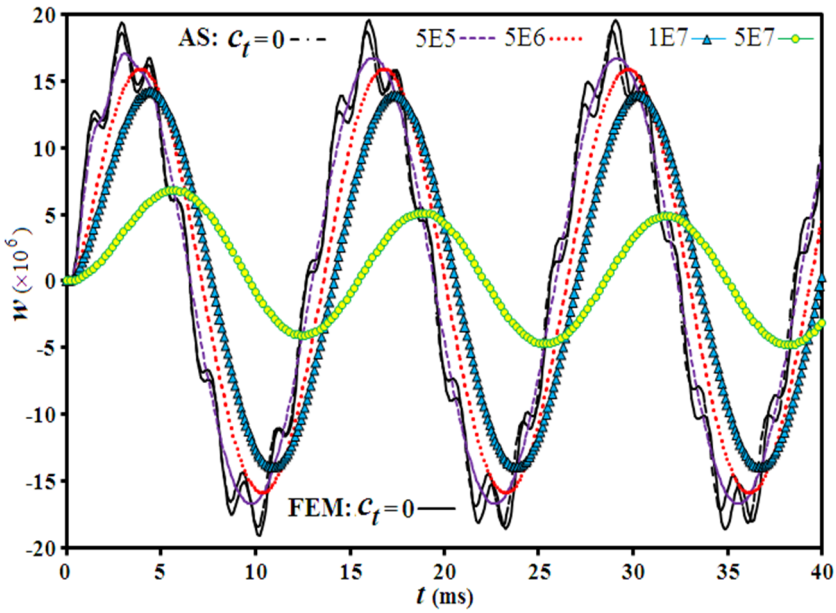

(d)

Figure 5: Dynamic response of clamped-free sandwich annular plate subjected to a uniform transverse load whose intensity varies according to a sinusoidal function (Case (III)): (a) $\omega = \Omega$, (b) $\omega = \Omega / 4$ (c) $\omega = \Omega / 6$ (d) $\omega = \Omega / 8$.

5.2 Transient Response of Functionally Graded Polar Orthotropic Sandwich Plate

In the present section, dynamic responses of circular sandwich plate fabricated from functionally graded polar orthotropic face sheets are investigated for various edge conditions. Also, effects of

stiffness and damping coefficients of viscoelastic foundation on the transient response of sandwich plate are examined for various dynamic loads.

Variation of the Young's modulus (in the radial and circumferential direction), shear modulus and density of each face sheet in the radial direction are chosen as:

a) Top face sheet:

$$\begin{Bmatrix} E_r^{(1)}(r) \\ E_\theta^{(1)}(r) \\ G_{rz}^{(1)}(r) \\ \rho^{(1)}(r) \end{Bmatrix} = \begin{Bmatrix} 170\,\text{GPa} \\ 68\ \text{GPa} \\ 34\ \text{GPa} \\ 1413/g\ \ \text{N/m}^3 \end{Bmatrix} \left[1 + 0.4\left(r - r_o\right)\right]$$

b) Bottom face sheet:

$$\begin{Bmatrix} E_r^{(3)}(r) \\ E_\theta^{(3)}(r) \\ G_{rz}^{(3)}(r) \\ \rho^{(3)}(r) \end{Bmatrix} = \begin{Bmatrix} 68\ \text{GPa} \\ 170\ \text{GPa} \\ 18\ \text{GPa} \\ 1413/g\ \ \text{N/m}^3 \end{Bmatrix} \left[1 + 0.7\left(r - r_o\right)\right]$$

Also, the Poisson's ratios are assumed as: $v_{r\theta}^{(1)} = 0.35,\ v_{r\theta}^{(3)} = 0.14$ where $\dfrac{v_{r\theta}}{E_{r\theta}} = \dfrac{v_{\theta r}}{E_{\theta r}}$

Dynamic responses of clamped-simply supported sandwich plate subjected to load cases (I), (IV) and (V) are plotted in figures 6-8, respectively. In these figures, time variations of the lateral deflection are presented for r=0.5. It is evident that the effects of elastic foundation (Winkler-type foundation) can be examined when damping coefficient C_t is set to zero. Figure 6 shows that vibration amplitude and frequency of plate under elastic foundation (C_t=0 and k_w=2E10) decreases and increases, respectively, comparing with those of the plate without foundation. The plate oscillates about the static value of deflection when there is no damping in the foundation (C_t =0), in which the vibration amplitude is constant. Also, the vibration amplitude of plate under viscous foundation decreases with time and tends to the static response of plate for C_t =0.

It can be seen from figure 7 that for sandwich plate subjected to an N-shaped pulse loading, the center of oscillation decreases with time and becomes negative when $t < \tau$ (forced vibration), when the load is removed ($t > \tau$ free vibration) the plate oscillates about the zero. As expected, vibration amplitude of plate without damping (C_t =0) is constant in each stage, but for plate subjected to a pulse loading rested on viscous foundation, the amplitude decreases with time and the lateral deflection tends to zero. Also for plate without foundation (C_t=k_w=0), vibration amplitude in the first stage ($t < \tau$) is higher than that of the second stage ($t > \tau$), but for plate under elastic foundation with C_t=0 and k_w=2E10, vibration amplitude in the second stage is higher. Indeed, in the first stage, vibration amplitude of plate without foundation is higher than that in the other cases and in the second stage, vibration amplitude of plate with C_t=0 and k_w=2E10 is higher.

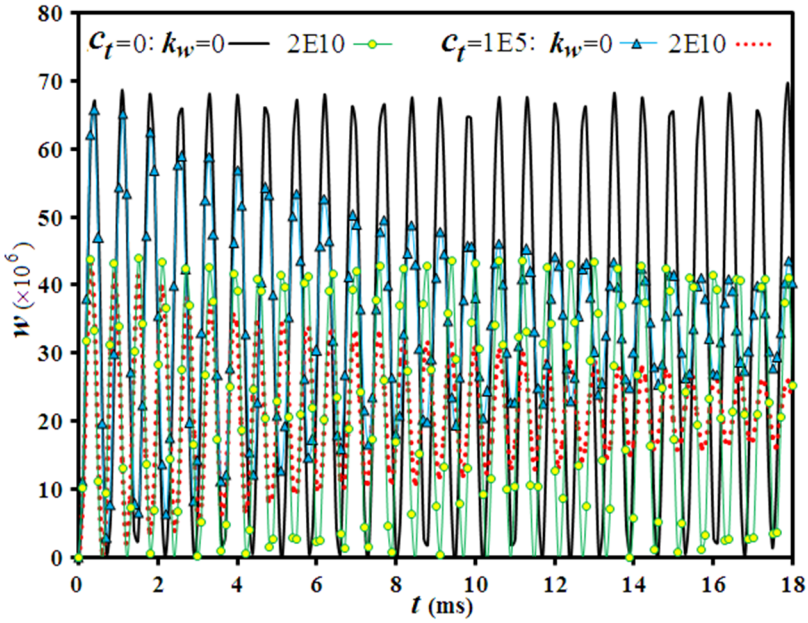

Figure 6: Dynamic response of clamped-simply supported sandwich annular plate subjected to an abrupt uniformly distributed transverse load (case (I)).

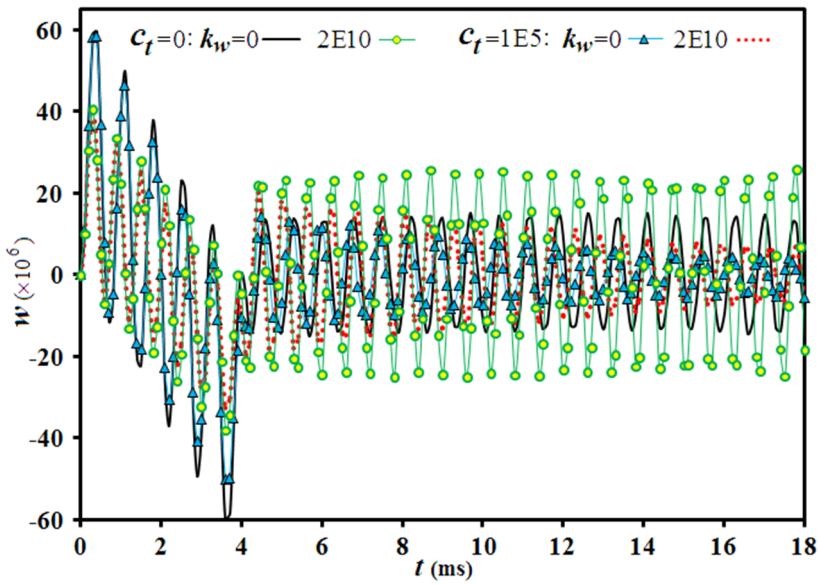

Figure 7: Dynamic response of clamped- simply supported sandwich annular plate subjected to an N-shaped pulse loading (case (IV)).

Figure 8 shows that for the plate subjected to load case (V), the response to the loading with $\tau = 2ms$ is higher than the response to the loading with $\tau = 4ms$. In the other words, the loading with the higher frequency of excitation leads to higher response.

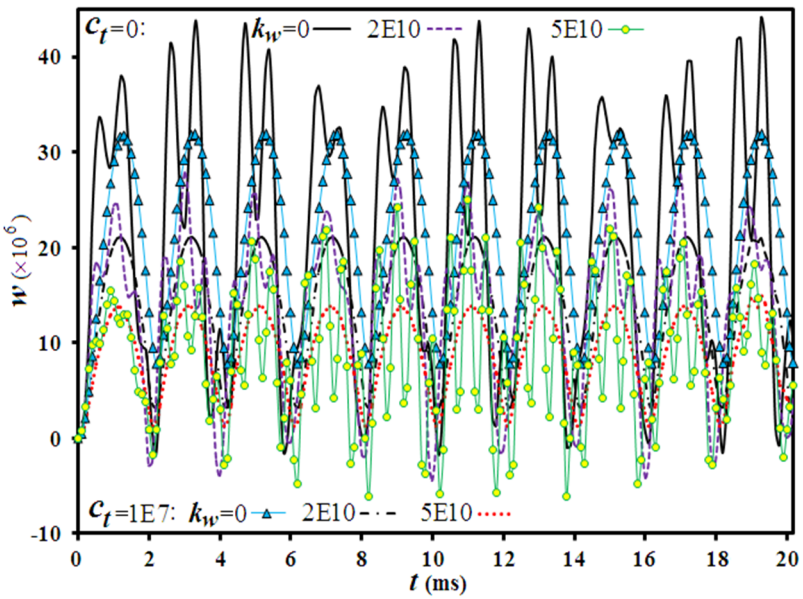

(a)

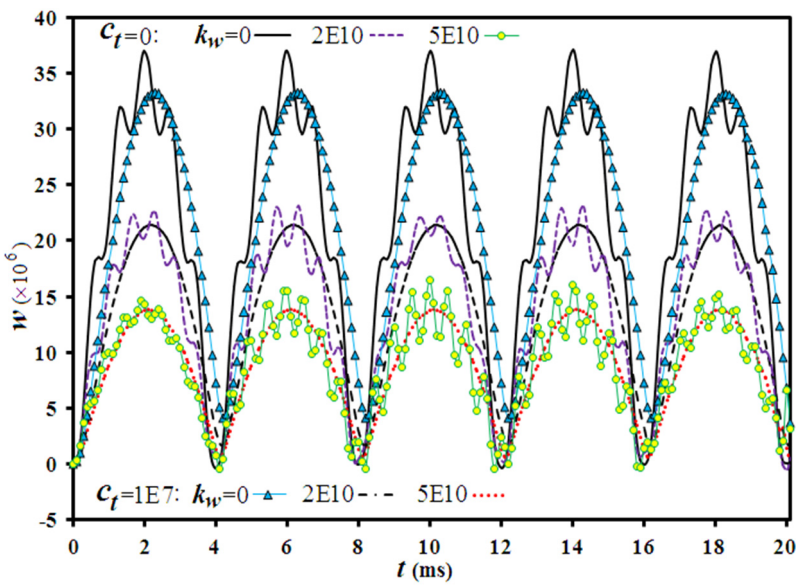

(b)

Figure 8: Dynamic response of clamped-simply supported sandwich annular plate subjected to a sinusoidal loading acting in the same direction (case (V)) with time duration: (a) $\tau = 2$ ms and (b) $\tau = 4$ ms.

This figure also shows that influence of other vibration modes which are superimposed on the main response of plate in undamped system, are eliminated for plates resting on the viscous foundation.

Effects of viscoelastic foundation on the dynamic response of clamped-clamped sandwich plate subjected to load cases (I), (VI) and (VII) are presented in figures 9-11, respectively. In these fig-

ures, the results are reported for r=0.5. It can be seen that in comparison with the forgoing example, there is a same trend for the dynamic response of sandwich plate under step loading with clamped-clamped and clamped-simply supported boundary conditions (figures 6 and 9). However, the vibration amplitude and frequency of clamped-clamped plate decreases and increases, respectively, comparing with those of the clamped-simply supported plate due to increasing the stiffness of plate with clamped-clamped edges.

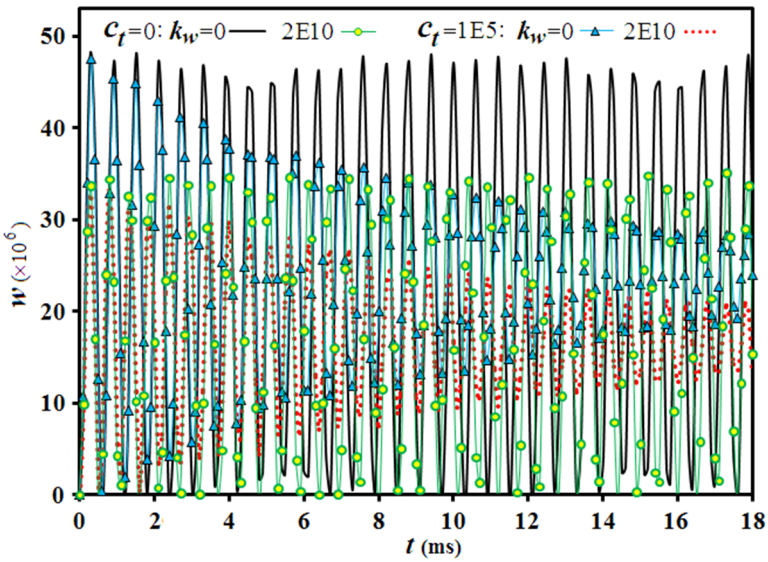

Figure 9: Dynamic response of clamped-clamped sandwich annular plate subjected to an abrupt uniformly distributed transverse load (case (I)).

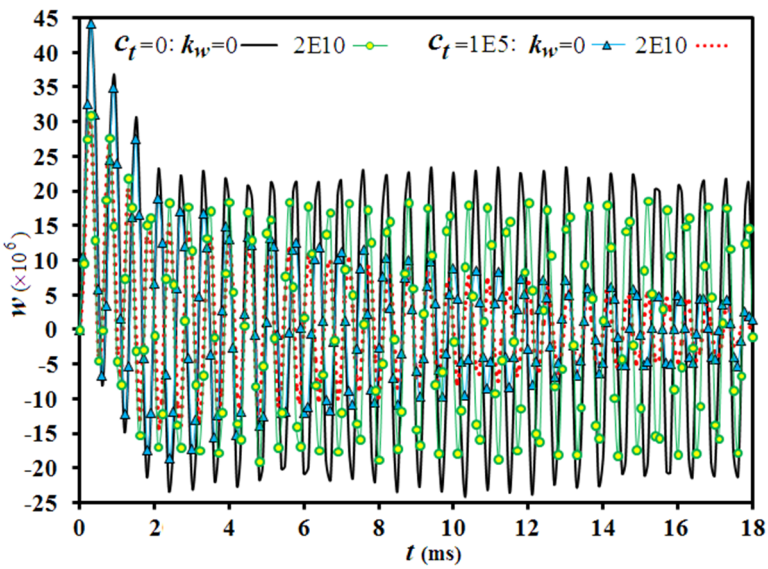

Figure 10: Dynamic response of clamped-clamped sandwich annular plate subjected to a triangular-shaped pulse loading (case (VI)).

It is observed that for dynamic response of plate under the triangular-shaped pulse and exponential loadings (figures 10 and 11), the center of oscillation decreases and approaches zero as time increases. These figures show that the vibration amplitude of plate without foundation (C_t=k_w=0) is higher than that in the other cases.

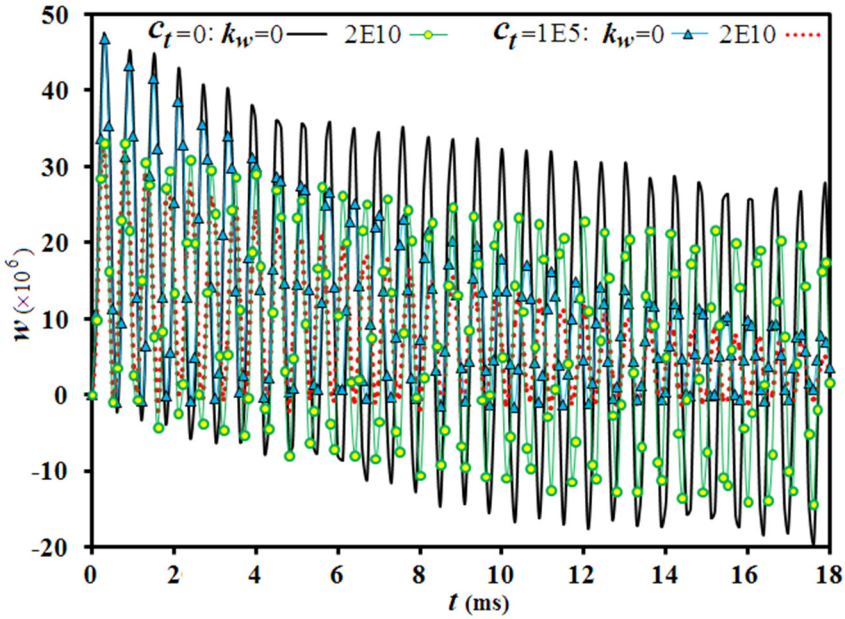

(a)

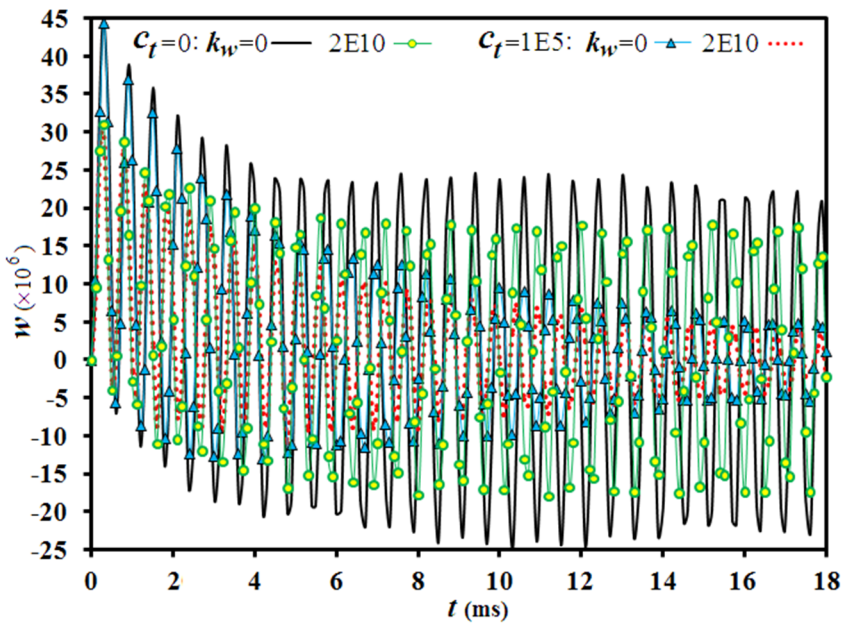

(b)

Figure 11: Dynamic response of clamped-clamped sandwich annular plate subjected to an exponential loading (case (VII)): (a) $\zeta = 100$ (b) $\zeta = 500$.

Time variations of the lateral deflection at the outer edge of the sandwich plate with clamped-free boundary condition subjected to load cases (VIII) and (IX) are plotted in figure 12 and 13, respectively. In figure 12, results of sandwich plate under repeated rectangular-shaped loading (load case (VII)) with time duration of 2ms and 4ms are illustrated.

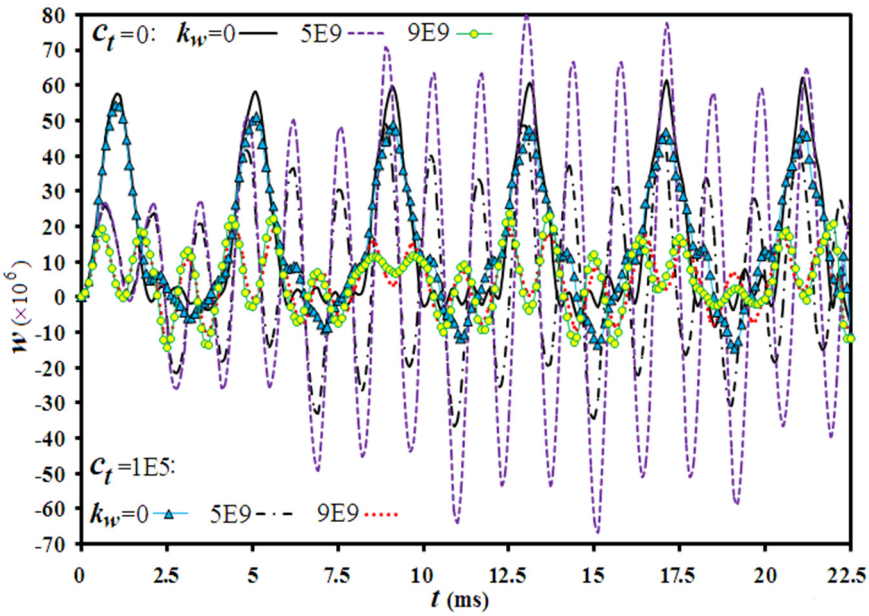

(a)

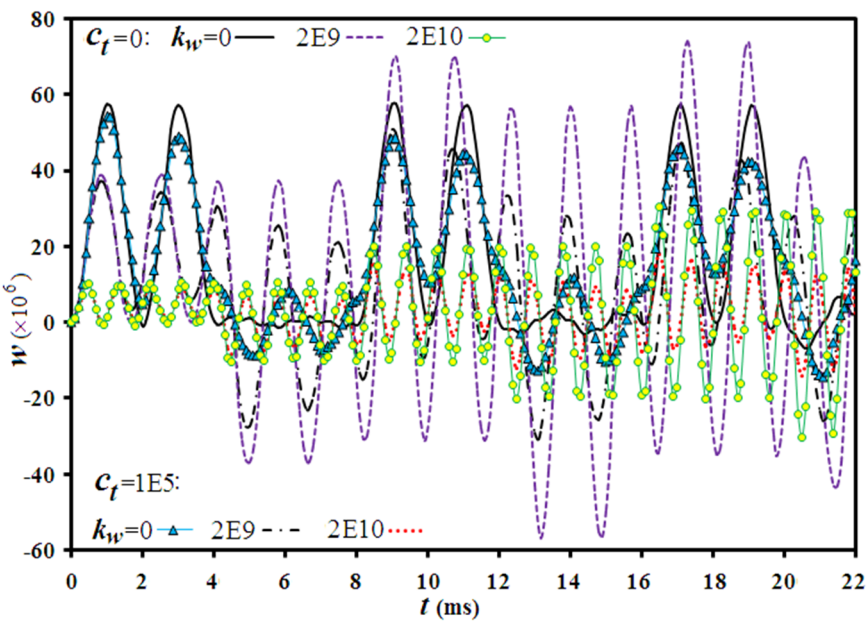

(b)

Figure 12: Dynamic response of clamped-free sandwich annular plate subjected to a repeated rectangular-shaped loading (Case (VIII)) with time duration: (a) $\tau = 2$ ms and (b) $\tau = 4$ ms.

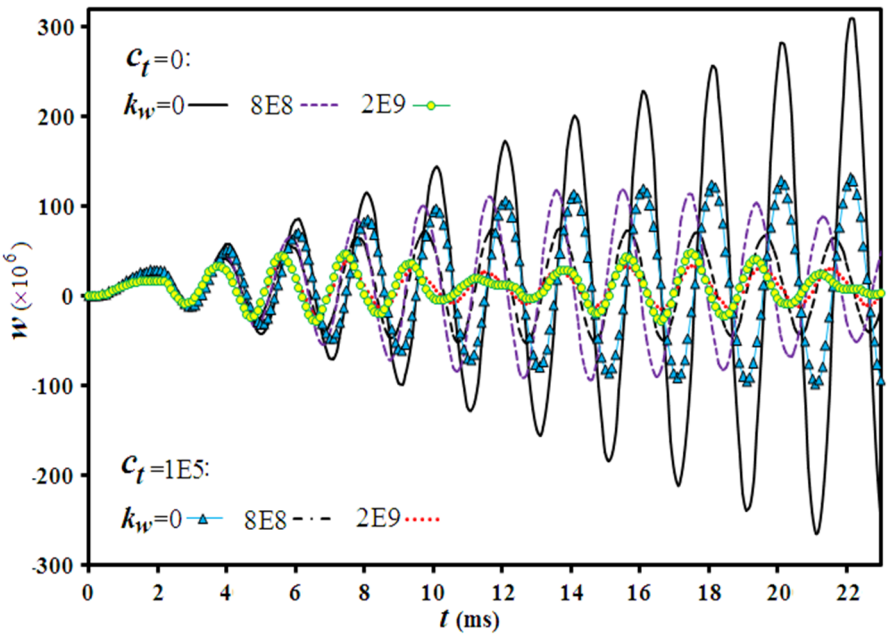

(a)

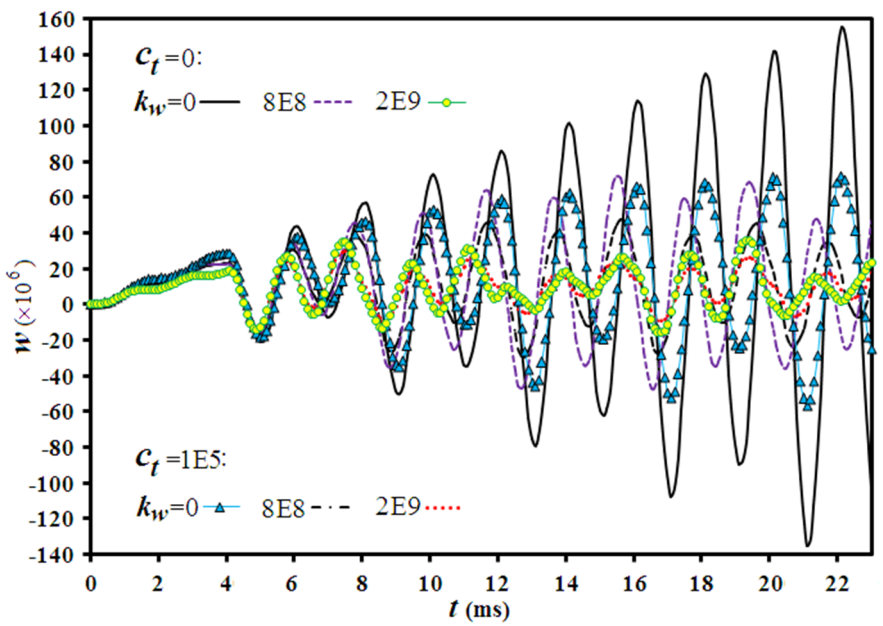

(b)

Figure 13: Dynamic response of clamped-free sandwich annular plate subjected to a repeated triangular-shaped loading (Case (IX)) with time duration: (a) $\tau = 2$ ms and (b) $\tau = 5$ ms.

It can be seen that in the first duration of loading ($t < \tau$), the peak deflection of plate without foundation is higher than the other cases and then ($t > \tau$) the peak deflection of plate under elastic foundation with K_w=5E9 in figure 12(a) and K_w=2E9 in figure 12(b) is higher. Increasing elastic

foundation stiffness value up from 5E9 to 9E9 in figure 12(a) and 2E9 to 2E10 in figure 12(b), causes an obvious decrease of vibration amplitude.

It is interesting to note that the viscoelastic foundation causes a reduction in the vibration amplitude of plate in the loading time durations $(2i\tau < t < (2i+1)\tau \;\; i = 0,1,2,\ldots)$, but in the time durations when the load is removed $((2i+1)\tau < t < 2(i+1)\tau \;\; i = 0,1,2,\ldots)$, the vibration amplitude of plate without foundation is smaller and its response is smoother.

Figure 13 shows that the oscillation amplitude of plate subjected to the repeated triangular-shaped loading is unbounded in undamped system. It is seen that the repeated triangular-shaped loading with lower time durations (τ) increases the amplitude rapidly. Also, vibration amplitude of plate under viscoelastic foundation is bounded in some cases of viscoelastic foundation, where the stiffness and viscosity coefficients of foundation become higher than specific values.

6 CONCLUSIONS

By using the layerwise theory, effects of the viscoelastic foundation on the dynamic response of sandwich annular plates are studied. The viscoelastic substrate is modeled as Kelvin-Voigt foundation. Sandwich plates may be fabricated from functionally graded polar orthotropic face sheets, where Young's modulus in the radial and circumferential direction, shear modulus and density of each face sheet may be varied continuously in the radial direction. The relatively complicated second order coupled partial differential equations are solved based on a developed semi-analytical solution procedure by using a combination of the finite Taylor's transform procedure in the space domain and the fourth-order Runge-Kutta method in the time domain. The results are obtained for various dynamic loads and edge conditions. For some special cases, the obtained results based on the proposed solution procedure are compared with finite element results based on the three dimensional theory of elasticity. The comparisons show that there is a very good agreement between present results and results of the three-dimensional theory of elasticity. Results reveal that FG polar orthotropic sandwich plates under various transient loads, edge conditions and foundation parameters may be analyzed by using the proposed solution procedure. Results also show that influence of other vibration modes which are superimposed on the main response of plate in undamped system, are eliminated for plates resting on the viscous foundation.

References

Alipour, M.M., (2016a). A novel economical analytical method for bending and stress analysis of functionally graded-sandwich circular plates with general elastic edge conditions, subjected to various loads, Composite Part B: Engineering95: 48-63.

Alipour, M.M., (2016b). Effects of elastically restrained edges on FG sandwich annular plates by using a novel solutionprocedure based on layerwise formulation, Archives of Civil and Mechanical Engineering 16: 678-694.

Alipour, M.M. (2016c). An analytical approach for bending and stress analysis of cross/angle-ply laminated composite plates under arbitrary non-uniform loads and elastic foundations, Archives of Civil and Mechanical Engineering 16(2): 193-210.

Alipour, M.M. (2018). Transient forced vibration response analysis of heterogeneous sandwich circular plates under viscoelastic boundary support, Archives of Civil and Mechanical Engineering 18: 12-31.

Alipour, M.M., Shariyat, M. (2015). Analytical zigzag formulation with 3D elasticity corrections for bending and stress analysis of circular/annular composite sandwich plates with auxetic cores, Composite Structures 132: 175-197.

Carrera, E., Brischetto, S. (2008). A survey with numerical assessment of classical and refined theories for the analysis of sandwich plates. Applied Mechanics Reviews 62(1): 010803–010819.

Ding, H., Shi, K.L., Chen, L.Q., Yang, S.P. (2013). Dynamic response of an infinite Timoshenko beam on a nonlinear viscoelastic foundation to a moving load, Nonlinear Dynamics 73: 285–298.

Ghashochi-Bargh, H., Sadr, M.H., (2014). Vibration reduction of composite plates by piezoelectric patches using a modifiedartificial bee colony algorithm, Latin American Journal of Solids and Structures 11: 1846-1863.

Ghorbanpour Arani, A., Shiravand, A., Rahi, M., Kolahchi, R., (2012). Nonlocal vibration of coupled DLGS systems embedded on Visco-Pasternak foundation, Physica B. 407: 4123–4131.

Ghorbanpour Arani, A., Maboudi, M.J., Kolahchi, R. (2014), Nonlinear vibration analysis of viscoelastically coupled

DLAGS-systems. European Journal of Mechanics - A/Solids 45: 185-197.

Hoang, T., Duhamel, D., Foret, G., Yin, H.P., Cumunel, G., (2016). Response of a periodically supported beam on a nonlinearfoundation subjected to moving loads, Nonlinear Dynamics 86(2): 953-961.

Hosseini Hashemi, S.h., Mehrabani, H., Ahmadi-Savadkoohi, A., (2015). Forced vibration of nanoplate on viscoelastic substrate with consideration of structural damping: An analytical solution, Composite Structures 133: 8-15.

Houari, M. S. A., Tounsi, A., Bég O. A., (2013). Thermoelastic bending analysis of functionally graded sandwich plates using a new higher order shear and normal deformation theory, International Journal of Mechanical Sciences 76: 102-111

Karim, K.R., Chen, G.D., (2012). Surface damping effect of anchored constrained viscoelastic layers on the flexural response of simply supported structures, Mechanical Systems and Signal Processing 27: 419–432.

Kiasat, M.S., Zaman, H.A., Aghdam, M.M., (2014). On the transient response of viscoelastic beams and plates on viscoelasticmedium, International Journal of Mechanical Sciences 83: 133–145.

Kim, S.M., McCullough, B.F., (2003). Dynamic response of plate on viscous Winkler foundation to moving loads of varyingamplitude, Engineering Structures 25: 1179–1188.

Lee, K.H., Cao, L., (1996). A predictor-corrector zig-zag model for the bending of laminated composite plates, InternationalJournal of Solids Structures 33(6): 879-897.

Lepoittevin, G., Kress, G., (2011). Finite element model updating of vibrating structures under free–free boundary conditionsfor modal damping prediction, International Journal of Mechanical Sciences 25: 2203–2218.

Liang, X.u., Wang, Z., Wang, L., Liu, G., (2014). Semi-analytical solution for three-dimensional transient response of functionallygraded annular plate on a two parameter viscoelastic foundation, Journal of Sound and Vibration 333: 2649-2663.

Luo, W.L., Xia, Y., Zhou, X.Q., (2016). A closed-form solution to a viscoelastically supported Timoshenko beam under harmonicline load, Journal of Sound and Vibration 369: 109-118.

Luong-Van, H., Nguyen-Thoi, T., Liu, G.R., Phung-Van, P., (2014). A cell-based smoothed finite element method usingthree-node shear-locking free Mindlin plate element (CS-FEM-MIN3) for dynamic response of laminated compositeplates on viscoelastic foundation, Engineering Analysis with Boundary Elements 42: 8–19.

Mazilu, T., Dumitriu, M., Tudorache, C., (2012). Instability of an oscillator moving along a Timoshenko beam on viscoelasticfoundation, Nonlinear Dynamics 67: 1273–1293.

Metrikine, A.V., Verichev, S.N., (2001). Instability of vibrations of a moving two-mass oscillator on a flexibly supported

Timoshenko beam, Archives of Civil and Mechanical Engineering 71: 613-624.

Mohammadimehr, M., Navi, B.R., Arani, A.G., (2015). Free vibration of viscoelastic double-bonded polymeric nano-compositeplates reinforced by FG-SWCNTs using MSGT, sinusoidal shear deformation theory and meshless method, CompositeStructures 13: 654-671.

Nie, G.J., Batra, R.C., (2010). Static deformations of functionally graded polar-orthotropic cylinders with elliptical innerand circular outer surfaces, Composites Science and Technology 70: 450-457.

Pan, Q., Tian He, T., Xiao, D., Liu, X., (2016). Design and Damping Analysis of a New Eddy Current Damper for AerospaceApplications, Latin American Journal of Solids and Structures 13: 1997-2011

Peng, X.L., Li, X.F., (2012). Elastic analysis of rotating functionally graded polar orthotropic disks, International Journal ofMechanical Sciences 60: 84–91.

Plattenburg, J., Dreyer, J. Singh, T. R., (2016). A new analytical model for vibration of a cylindrical shell and card-boardliner with focus on interfacial distributed damping. Mechanical Systems and Signal Processing 75: 176–195.

Pouresmaeeli, S., Ghavanloo, E., Fazelzadeh, S.A., (2013). Vibration analysis of viscoelastic orthotropic nanoplates restingon viscoelastic medium. Composite structures 96: 405–410.

Reddy, J. (2006). An introduction to the Hinite element method. 2ndEdition, New York: Wiley.

Shariyat, M., Alipour, M.M., (2015). Novel Layerwise Shear Correction Factors for Zigzag Theories of Circular SandwichPlates with Functionally Graded Layers, Latin American Journal of Solids and Structures 12: 1362-1396.

Shariyat, M., Alipour, M.M., (2017a). Analytical layerwise free vibration analysis of circular/annular composite sandwichplates with auxetic cores, International Journal of Mechanics and Materials in Design 13, 125-157.

Shariyat, M., Alipour, M.M., (2017b). Analytical bending and stress analysis of variable thickness FGM auxetic conical/cylindrical shells with general tractions, Latin American Journal of Solids and Structures 14: 805-843.

Tounsi, A., Houari, M. S. A.,Benyoucef, S.,Bedia, E. A. A., (2013). A refined trigonometric shear deformation theory for thermoelastic bending of functionally graded sandwich plates, Aerospace Science and Technology24 (1): 209-220.

Yang, Y., Ding, H., Chen, L.Q., (2013). Dynamic response to a moving load of a Timoshenko beam resting on a nonlinearviscoelastic foundation, Acta Mechanica Sinica 29(5): 718-727.

Zamani H.A., Aghdam, M.M., Salehi, M., (2017). Free damped vibration analysis of Mindlin plates with hybrid material foundation viscoelasticity. International Journal of Mechanical Sciences, 121: 33–43.

Zenkour, A.M., (2016). Nonlocal transient thermal analysis of a single-layered graphene sheet embedded in viscoelas-tic medium, Physica E 79: 87-97.

Zhang, D.P., Lei, Y., Shen, Z.B., (2016). Free transverse vibration of double-walled carbon nanotubes embedded in viscoelastic médium, Acta Mechanica 227(12): 3657–3670.